

Imaging of Uncommon Retroperitoneal Masses¹

CME FEATURE

See www.rsna.org/education/lrg_cme.html

LEARNING OBJECTIVES FOR TEST 3

After reading this article and taking the test, the reader will be able to:

- Describe the various solid and cystic retroperitoneal masses.
- Recognize the imaging features of various retroperitoneal masses.
- Discuss some of the specific imaging features that can narrow the differential diagnosis of retroperitoneal masses.

TEACHING POINTS

See last page

Prabhakar Rajiah, MBBS, MD, FRCR • Rakesh Sinha, MD, FRCR
Carlos Cuevas, MD • Theodore J. Dubinsky, MD • William H. Bush, Jr, MD
Orpheus Kolokythas, MD

Retroperitoneal masses not arising from major solid organs are uncommon. Although there is no simple method of classifying retroperitoneal masses, a reasonable approach is to consider the masses as predominantly solid or cystic and to subdivide these into neoplastic and non-neoplastic masses. Because the treatment options vary, it is useful to be able to differentiate these masses by using imaging criteria. Although the differential diagnosis of retroperitoneal masses can be narrowed down to a certain extent on the basis of imaging characteristics, patterns of involvement, and demographics, there is still a considerable overlap of imaging findings for these masses, and histologic examination is often required for definitive diagnosis. Computed tomography (CT) and magnetic resonance (MR) imaging play an important role in characterization and in the assessment of the extent of the disease and involvement of adjacent and distant structures. Familiarity with the CT and MR imaging features of various retroperitoneal masses will facilitate accurate diagnosis and staging for aggressive lesions.

Introduction

Primary retroperitoneal masses, which originate in the retroperitoneum but outside the major retroperitoneal organs, are uncommon and can be divided primarily into solid and cystic masses, each of which can be further subdivided into neoplastic and nonneoplastic masses (Tables 1, 2). **Of the primary retroperitoneal neoplasms, 70%–80% are malignant in nature, and these account for 0.1%–0.2% of all malignancies in the body (1,2).** Because the treatment options vary, it is useful to be able to noninvasively distinguish these masses. Computed tomography (CT) and magnetic resonance (MR) imaging play an important role in characterization (size, shape, wall thickness, septa, calcification, and fat content) and the assessment of the extent of the disease and involvement of adjacent and distant structures (1,3,4). Although CT is best for assessing calcification, MR imaging has superior soft-tissue contrast, which is useful for staging and the assessment of vascular invasion, as well as for evaluating the fat content of lesions. Ultrasonography (US) plays a relatively limited role in the evaluation of masses, except for the

Teaching Point

Abbreviations: FDG = fluorine 18 fluorodeoxyglucose, IVC = inferior vena cava, STIR = short inversion time inversion-recovery

RadioGraphics 2011; 31:949–976 • Published online 10.1148/rg.314095132 • Content Codes: GI OI

¹From the Imaging Institute, Cleveland Clinic Foundation, 9500 Euclid Ave, Cleveland, OH 44195 (P.R.); Warwick Hospital, South Warwickshire NHS Trust and Warwick Medical School, Warwick, England (R.S.); and the Department of Radiology, University of Washington Medical Center, Seattle, Wash (C.C., T.J.D., W.H.B., O.K.). Presented as an education exhibit at the 2008 RSNA Annual Meeting. Received June 19, 2009; revision requested September 16 and received September 26, 2010; accepted October 11. For this journal-based CME activity, the authors (P.R., R.S., W.H.B.), editor, and reviewers have no relevant relationships to disclose. C.C. received a research grant from Merck; T.J.D. is a consultant for ConnexMD; O.K. received a grant from and is a consultant and is on the Advisory Board for Koninklijke Philips Electronics. **Address correspondence to P.R.** (e-mail: radprabhakar@gmail.com).

Table 1
Classification of Solid Retroperitoneal Masses

Type of Mass, Origin, and Cell of Origin	Benign	Malignant
Neoplastic		
Mesodermal origin		
Adipose tissue	Lipoma	Liposarcoma
Smooth muscle	Leiomyoma	Leiomyosarcoma
Connective tissue	Fibroma	Malignant fibrous histiocytoma, fibrosarcoma, chondrosarcoma, synovial cell sarcoma
Striated muscle	Rhabdomyoma	Rhabdomyosarcoma
Blood vessels	Hemangioma, hemangiopericytoma	Angiosarcoma
Perivascular epithelioid cells	Perivascular epithelioid cell tumor (PEComa) group: angiomyolipoma, lymphangi leiomyomatosis, clear cell "sugar" tumor, clear cell myo-melanocytic tumor, pigmented melanotic tumor	Sarcoma of perivascular cells
Interstitial cells of Cajal	Gastrointestinal stromal tumor (GIST)	...
Primitive mesenchyme	Myxoma	Myxosarcoma
Notochordal remnant	Chordoma	...
Miscellaneous	Myelolipoma, fibromatosis, angiomyofibroblastoma	...
Uncertain	Xanthogranuloma	...
Neurogenic origin		
Nerve sheath	Schwannoma, neurofibroma	Malignant schwannoma, neurogenic sarcoma, neurofibrosarcoma
Sympathetic nerves	Ganglioneuroma, ganglioneuroblastoma	Neuroblastoma
Chromaffin tissue	Paraganglioma, pheochromocytoma	Malignant paraganglioma or pheochromocytoma
Germ cell, sex cord, and stromal cell origin		
Germ cell	Mature teratoma, immature teratoma	Seminoma, malignant teratoma, embryonal carcinoma, yolk sac tumor, choriocarcinoma, mixed germ cell tumor
Sex cord stromal	Granulosa cell tumor, thecoma, Sertoli-Leydig cell tumor	...
Lymphoid or hematologic origin	...	Lymphoma, posttransplant lymphoproliferative disease, extramedullary plasmacytoma
Nonneoplastic*		
*Nonneoplastic masses include pseudotumoral lipomatosis, retroperitoneal fibrosis, Erdheim-Chester disease, and extramedullary hematopoiesis.		

assessment of vascular invasion, which could be performed better with CT and MR imaging. The differential diagnosis of retroperitoneal masses can be narrowed down to a certain extent on the basis of imaging characteristics, patterns of involvement, and demographics;

however, there is a substantial overlap of imaging findings, and histologic examination is often required for definitive diagnosis.

The purpose of this article is to review the imaging features of various uncommon retroperitoneal masses, with emphasis on the CT and MR imaging findings. First, the anatomy of the retroperitoneum is briefly reviewed. Then solid retro-

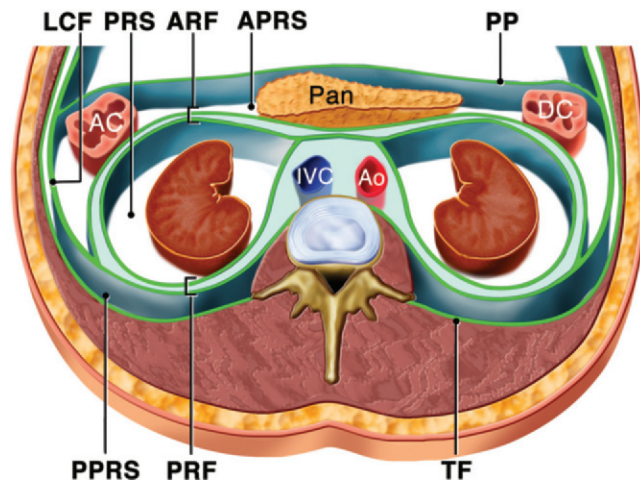


Figure 1. Drawing of the anatomy of the retroperitoneal spaces at the level of the kidneys. The anterior pararenal space (*APRS*) is located between the parietal peritoneum (*PP*) and the anterior renal fascia (*ARF*) and contains the pancreas (*Pan*), the ascending colon (*AC*), and the descending colon (*DC*). The posterior pararenal space (*PPRS*) is located between the posterior renal fascia (*PRF*) and the transversalis fascia (*TF*). The perirenal space (*PRS*) is located between the anterior renal fascia and the posterior renal fascia. *Ao* = aorta, *IVC* = inferior vena cava, *LCF* = lateroconal fascia.

Table 2
Classification of Cystic Retroperitoneal Masses

Type of Mass and Origin	Mass
Neoplastic	
Epithelial	Mucinous cystadenoma or cystadenocarcinoma, serous cystadenocarcinoma
Mesothelial	Mesothelioma
Germ cell	Cystic teratoma
Cystic change in solid neoplasm	Paraganglioma, neurilemoma, sarcoma
Miscellaneous	Lymphangioma, lymphangiomatosis, lymphangiomyoma, müllerian cyst, epidermoid cyst, tailgut cyst, bronchogenic cyst, pseudomyxoma retroperitonei, perianal mucinous cystadenocarcinoma
Nonneoplastic	
	Hematoma, urinoma, lymphocele, pancreatic pseudocyst, nonpancreatic pseudocyst

peritoneal masses are covered, grouped into solid neoplastic masses and solid nonneoplastic masses. Cystic retroperitoneal masses are presented next, grouped into cystic neoplastic masses and cystic nonneoplastic masses. Finally, diagnostic clues for retroperitoneal masses are reviewed.

Anatomy of the Retroperitoneum

The retroperitoneum extends from the diaphragm superiorly to the pelvis inferiorly and is situated between the posterior parietal peritoneum anteriorly and the transversalis fascia posteriorly. The retroperitoneum is broadly divided into the anterior and posterior pararenal, perirenal, and great vessel spaces. The anterior pararenal space is bordered anteriorly by the posterior parietal peritoneum, posteriorly by the anterior renal fascia (Gerota fascia), and laterally by the lateroconal fascia (Fig 1). The anterior pararenal space is subdivided into the pancreaticoduodenal space, which contains the pancreas and duode-

num, and the pericolonic space, which contains the ascending and descending colon.

The posterior pararenal space is situated between the posterior renal fascia (Zuckerkindl fascia) (5) and the transversalis fascia, whereas the perirenal space is located between the anterior renal fascia and the posterior renal fascia. The great vessel space is the fat-containing region that surrounds the aorta and the inferior vena cava (IVC) and lies anterior to the vertebral bodies and psoas muscles. Below the level of the kidneys, the anterior and posterior pararenal spaces merge to form the infrarenal retroperitoneal space, which communicates inferiorly with the prevesical space and extraperitoneal compartments of the pelvis (6–8). Because of loose connective tissue in the retroperitoneum, tumors can have widespread extension before clinical presentation (2).



Figure 2. Liposarcoma: various patterns on axial contrast-enhanced CT images. **(a)** Well-differentiated liposarcoma in a 58-year-old woman is shown as a large homogeneous fat-containing mass with thick septa (arrows) that show soft-tissue attenuation. **(b)** In a 65-year-old woman, mixed pattern is shown in a dedifferentiated liposarcoma that contains fat (arrowhead) and a large enhancing soft-tissue component (arrow). **(c)** Myxoid liposarcoma in the left side of the retroperitoneum in a 42-year-old man is shown as a large mass that has low attenuation and faint internal contrast enhancement (arrow). **(d)** Pleomorphic liposarcoma in the right retrocolic compartment of a 63-year-old man is shown as a solid soft-tissue mass (arrowhead) without any macroscopic fat.

Solid Neoplastic Masses

Solid neoplasms in the retroperitoneum can be broadly divided into four groups: *(a)* mesodermal neoplasms; *(b)* neurogenic tumors; *(c)* germ cell, sex cord, and stromal tumors; and *(d)* lymphoid and hematologic neoplasms.

Mesodermal Neoplasms

Retroperitoneal sarcomas constitute 0.1%–0.2% of all malignancies. Most of the retroperitoneal neoplasms are of mesodermal origin, with li-

posarcomas, leiomyosarcomas, and malignant fibrous histiocytomas making up more than 80% of these tumors. Retroperitoneal sarcomas are commonly seen in the 5th and 6th decades of life. These tumors are large at the time of clinical presentation and often involve adjacent structures. Compression of adjacent organs causes formation of a pseudocapsule. The recurrence rates are high, and metastases to liver, lung, bones, and brain may be seen (1,2).

Liposarcoma.—Liposarcoma is the most common (33%) primary retroperitoneal sarcoma (1).



Figure 3. Leiomyosarcoma in a 71-year-old woman. Axial CT image shows a large tumor with extensive areas of necrosis (arrow) in the left side of the retroperitoneum.

Ten to fifteen percent of liposarcomas occur in the retroperitoneum, and they are more common in the 50–70-year age group, with no sex predilection (1). Histologically, liposarcoma is classified, in increasing order of malignancy, into four subtypes: well-differentiated, myxoid, pleomorphic, and round cell subtypes. Various histologic subtypes may be seen in the same lesion (9,10). Liposarcoma is usually large (average diameter, >20 cm) and is a slow-growing tumor.

The well-differentiated subtype, the most common type of retroperitoneal liposarcoma (1), is a predominantly hypoattenuating lesion on CT images because of its fat content. At MR imaging, well-differentiated liposarcoma demonstrates high signal intensity on T1-weighted images and intermediate signal intensity on T2-weighted images. There is loss of fat signal intensity on fat-suppressed MR images. The appearance of liposarcoma may be similar to that of a lipoma, but liposarcoma has thicker, irregular, and nodular septa that show enhancement after contrast material administration (Fig 2a). Furthermore, lipoma is less common than liposarcoma in the retroperitoneum (9,11,12). Well-differentiated tumors can recur but do not metastasize. The fat in recurrent tumors has higher attenuation values than the normal retroperitoneal fat. Occasionally, a portion of the well-differentiated liposarcoma undergoes histologic dedifferentiation and becomes more aggressive and metastatic and then carries a worse prognosis. At CT and MR imaging, these dedifferentiated tumors are depicted as heterogeneous tumors with both fat and solid components and show a lack of clear delineation between solid and fat components. Calcification is seen in as many as 30% of cases and is an im-

portant sign of dedifferentiation. Variable signal intensity and enhancement of the solid portion may be seen (12) (Fig 2b).

Myxoid liposarcoma is seen in a younger population. At CT, the mass has a heterogeneous hypoattenuating appearance, with attenuation less than that of muscle. Homogeneous distribution of fat and soft tissue within the mass may result in a “pseudocystic” appearance (Fig 2c). At MR imaging, there is low signal intensity on T1-weighted images and high signal intensity on T2-weighted images because of the mucopolysaccharide contents in the myxoid matrix. Lacy, linear, or amorphous areas of high signal intensity on T1-weighted images and intermediate signal intensity on T2-weighted images may be seen because of the intratumoral fat content. Slowly progressive, reticular contrast enhancement that is due to the solid components enables differentiation from a cyst. A homogeneously hypoattenuating mass at CT that has a solid appearance at US is consistent with a myxoid tumor.

Pleomorphic and round cell liposarcomas are seen as heterogeneous soft-tissue masses (Fig 2d) with areas of necrosis that are indistinguishable from other solid tumors. Even in solid-appearing lesions, small foci of fat can be seen in as many as one-quarter of cases, particularly at MR imaging (12).

Leiomyosarcoma.—Leiomyosarcoma is the second most common (28%) primary retroperitoneal sarcoma (1). Leiomyosarcoma arises from retroperitoneal smooth muscle tissue, blood vessels, or wolffian duct remnants and can grow to a large size (>10 cm) before compromising adjacent organs and precipitating clinical symptoms such as venous thrombosis. Leiomyosarcoma is more common in women, in the 5th to 6th decades of life (13). Histopathologically, this tumor has large areas of necrosis and cystic degeneration, but calcification is uncommon. Leiomyosarcoma can be predominantly extravascular (62%) or intravascular (5%) in the retroperitoneum or can have a combination of extra- and intravascular components (33%). At CT, small tumors may be homogeneously solid, but large tumors have extensive areas of necrosis and occasional hemorrhage (Fig 3). Rarely, leiomyosarcoma may appear as mostly cystic. At MR imaging, these tumors have intermediate to low signal intensity on T1-weighted images and intermediate to high signal intensity on T2-weighted images, depending on the amount of necrosis. Mixed signal intensity and a

fluid-debris level can be seen in hemorrhagic lesions. **The presence of extensive necrosis in a retroperitoneal mass, with contiguous involvement of a vessel, is highly suggestive of leiomyosarcoma.** Metastasis to the liver, lungs, or lymph nodes occurs late in the course of the disease (1,13).

Approximately 6% of leiomyosarcomas arise from the IVC (1). Most of these tumors have a large extravascular component that makes it difficult to distinguish them from a secondary involvement of the IVC with an extrinsic tumor. The most commonly affected location is the segment between the diaphragm and renal veins. Tumors involving the superior segment of the IVC (above the hepatic veins) may manifest with Budd-Chiari syndrome, those of the middle segment (between the hepatic and renal veins) manifest with right upper quadrant pain or tenderness or the nephrotic syndrome, and tumors of the inferior segment (below the renal veins) manifest with pain and lower extremity edema (13). At CT, leiomyosarcoma of the IVC is depicted as an intermediate-attenuation mass with heterogeneous enhancement. Intraluminal masses result in expansion and obstruction of the IVC, and extraluminal masses cause extrinsic compression and proximal dilation (Fig 4). MR imaging typically shows an intraluminal intermediate-signal-intensity mass on T1- and T2-weighted images, with contrast enhancement. The differential diagnosis includes benign thrombus, angiosarcoma, and a tumor extending to the IVC from adjacent organs. While benign bland thrombus does not show any contrast enhancement, leiomyosarcoma of the IVC enhances on both early and delayed (10-minute) contrast-enhanced images and causes more expansion of the IVC (13,14). Tumors from the middle segment of the IVC have a better prognosis than those from other IVC segments (14).

Malignant Fibrous Histiocytoma.—Malignant fibrous histiocytoma is the third most common retroperitoneal sarcoma (19%) and overall is the most common soft-tissue sarcoma in the body. Malignant fibrous histiocytoma arises from primitive mesenchymal elements, and 15% of these tumors occur in the retroperitoneum (1). This tumor is more common in males (3:1), particularly in the 50–60-year age group. CT



Figure 4. Leiomyosarcoma with IVC involvement in a 53-year-old man. Axial T1-weighted spin-echo MR image shows a well-defined homogeneous mass with low signal intensity (straight arrow) and an absence of clear demarcation from the IVC (curved arrow). This feature is highly suggestive of leiomyosarcoma.

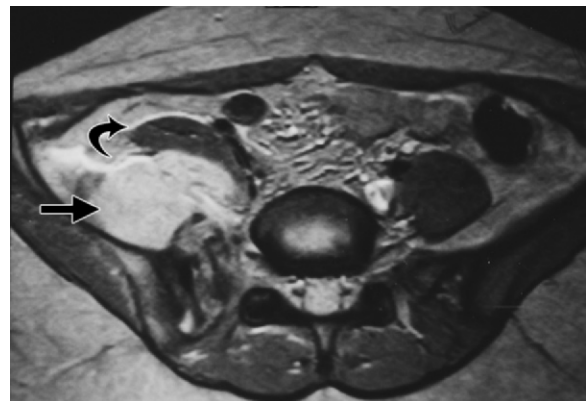


Figure 5. Malignant fibrous histiocytoma in a 49-year-old woman. Axial T2-weighted fast spin-echo MR image shows heterogeneous hyperintensity (straight arrow) within the mass, which is infiltrating the right psoas muscle (curved arrow).

and MR imaging appearances are nonspecific and demonstrate a large, infiltrating, and heterogeneously enhancing soft-tissue mass with areas of necrosis and hemorrhage and with invasion of adjacent organs (Fig 5). Variable patterns of calcification can be seen (7%–20% of cases) in the peripheral portions of these tumors. A cystic variant with peripheral calcification has been reported. The presence of calcification may help to distinguish malignant fibrous histiocytoma from leiomyosarcoma (1).

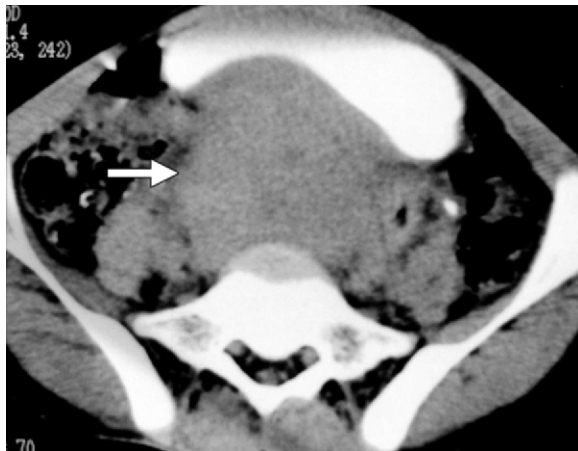


Figure 6. Rhabdomyosarcoma in a 12-year-old boy. Axial noncontrast CT image shows a large homogeneous mass (arrow) in the retroperitoneum. The mass is causing anterior displacement of the bladder.

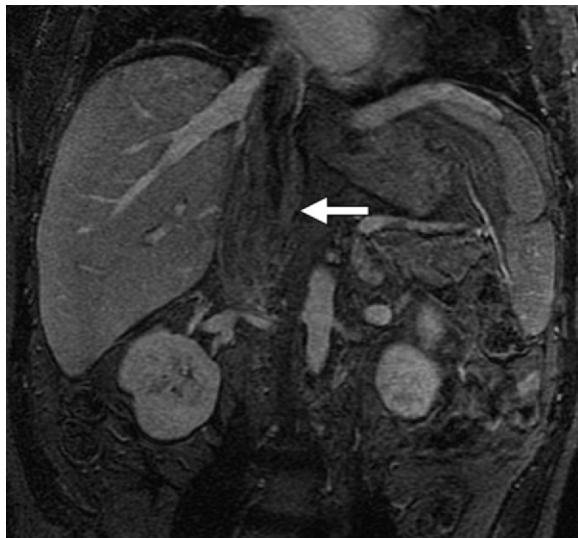


Figure 7. Angiosarcoma in a 61-year-old woman. Coronal contrast-enhanced T1-weighted fat-suppressed gradient-echo MR image shows that the IVC is expanded by a large intraluminal mass that shows heterogeneous enhancement (arrow). The findings from histopathologic examination indicated that the mass was an angiosarcoma of the IVC.

Less Common Sarcomas.—Rhabdomyosarcoma is a malignant tumor that arises from the primitive mesenchyme with rhabdomyoma differentiation. Rhabdomyosarcoma has a bimodal distribution in the pediatric population, with peaks in occurrence at 7 years and at adolescence (15). The retroperitoneum is involved in 7% of cases.

CT or MR imaging shows a mass lesion with areas of calcification, necrosis, and heterogeneous enhancement (Fig 6). Occasionally, high-flow blood vessels may be seen. Metastases occur in 10%–20% of rhabdomyosarcoma cases because of lymphatic or hematogenous spread.

Angiosarcoma is a malignant tumor of endothelial and mesenchymal cells. Most angiosarcomas occur in the right atrium, with less common involvement of the retroperitoneum, specifically the IVC. CT or MR imaging shows an enhancing mass expanding the involved vessel (Fig 7). MR imaging may show high signal intensity on T2-weighted images that is due to tumor necrosis and the presence of methemoglobin. Heterogeneous enhancement is demonstrated because of areas of necrosis (16).

Chondrosarcoma is a malignant tumor that produces cartilage matrix. Extraskeletal chondrosarcomas constitute 2% of all soft-tissue sarcomas and are extremely rare in the retroperitoneum (17). CT typically shows a large soft-tissue mass, which may have chondroid ring or arc type of calcifications. Amorphous punctate calcification may also be seen in the myxoid subtype. Serpentine flow voids may be seen on T2-weighted MR images. After contrast material administration, prominent diffuse heterogeneous enhancement may be seen (18).

Synovial cell sarcoma is commonly seen around the joints (85%–95% of cases) and is extremely rare in the retroperitoneum, a location where it is associated with a poor prognosis. Synovial cell sarcoma usually occurs in patients between 15 and 40 years of age, with no sex predilection (19). Imaging findings are nonspecific, but this tumor should be considered in the differential diagnosis when a young patient presents with a retroperitoneal mass. At CT, synovial cell sarcoma is hypoattenuating, with peripheral irregular enhancement and central areas of necrosis. Calcification, hemorrhage, or cyst formation with fluid-fluid levels can also be seen. MR imaging shows a heterogeneous mass, which is isointense on T1-weighted images and hyperintense on T2-weighted images. In 80% of patients, metastases are seen, mainly metastases to the lungs (20).

Perivascular Epithelioid Cell Tumor.—Perivascular epithelioid cell tumor (also called PEComa) is a mesenchymal tumor that is composed of distinctively perivascular epithelioid cells, which are radially arranged cells around a vascular lumen. The cells express melanocytic markers (melan-A, microphthalmia transcription factor) and smooth muscle markers (HMB-45, actin). These tumors are mostly benign but have varying malignant potential (21). The tumors included in this group are angiomyolipomas, lymphangioliomyomatosis, clear cell “sugar” tumors, clear cell myomelanocytic tumors, sarcoma of perivascular cells, and pigmented melanotic tumors.

Angiomyolipoma.—Angiomyolipoma has varying amounts of blood vessels, smooth muscle cells, and adipose tissue. The tumor can be asymptomatic or can manifest with hemorrhage. Angiomyolipoma is more common in females and can either be sporadic or associated with tuberous sclerosis. Angiomyolipoma occurs in a younger age group (25–35 years) and is bilateral when associated with tuberous sclerosis. Histopathologically, angiomyolipoma is unencapsulated and is predominantly composed of fat, with lesser amounts of blood vessels and smooth muscle. Angiomyolipoma is usually located in the kidneys but occasionally can be seen in the retroperitoneum, solid organs, skin, or gynecologic tract (12). At CT and MR imaging of angiomyolipomas, small tumors are homogeneous and larger tumors are heterogeneous soft-tissue masses that typically contain a large amount of macroscopic fat and hyperenhancing vascular soft tissue. Enlarged vessels coursing through the lesion (Fig 8), aneurysms, and associated hemorrhage are features that enable distinguishing an angiomyolipoma from liposarcoma (12). Hemorrhage is more common in larger tumors. Occasionally, a solid lesion without fat may be seen. (Lymphangioliomyoma is discussed in a section under “Cystic Neoplastic Masses.”)

Myelolipoma.—Myelolipoma is a benign tumor composed of hematopoietic cells and mature adipose tissue (22); the tumor is likely caused by (a) differentiation of primitive hematopoietic stem cell rests in response to a triggering stimulus or (b) embolization of bone marrow tissue.

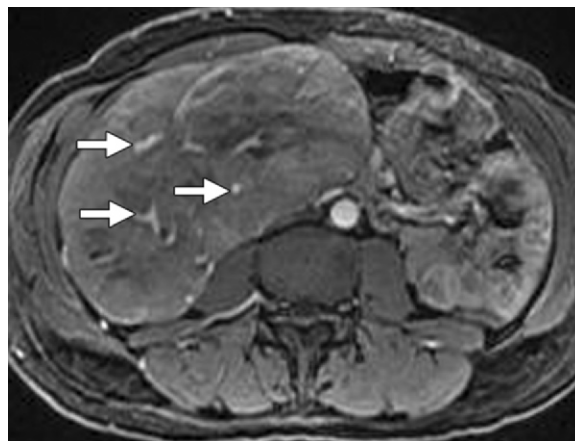


Figure 8. Perivascular epithelioid cell tumor (also called PEComa) in a 38-year-old man. Axial contrast-enhanced T1-weighted fat-suppressed gradient-echo MR image shows a retroperitoneal mass that contains intensely enhancing vessels (arrows). The findings from histopathologic examination disclosed that this mass was a perivascular epithelioid cell tumor, subtype angiomyolipoma.

Myelolipoma is usually asymptomatic but can manifest with discomfort or pain caused by hemorrhage or compression. Myelolipoma is more common in females, particularly in middle to old age. Histopathologically, myelolipoma is well encapsulated, and it has myeloid and erythroid precursors, with mature adipose tissue and occasionally hemorrhage and calcification (22). The adrenal glands are the most common location for myelolipoma. It is rarely seen in the retroperitoneum or presacral region (9).

At CT, myelolipoma is depicted as a heterogeneous mass with areas of fat and enhancing soft tissue (Fig 9). The attenuation value of fat in myelolipoma is higher than that of normal retroperitoneal fat because of the mixed hematopoietic tissue. Extraadrenal lesions contain less fat than adrenal lesions (50% vs 90%). Calcification and hemorrhage are seen in 10% of cases. At MR imaging, the fatty component has high signal intensity on T1-weighted images. Heterogeneous high signal intensity may be seen on T2-weighted images because of the admixture with hematopoietic tissue, myeloid tissue, and hemorrhage (22). Extraadrenal myelolipomas are difficult to distinguish from liposarcoma or other fat-containing tumors. Liposarcomas are less well defined, are unencapsulated, and are infiltrative without



Figure 9. Myelolipoma in a 44-year-old woman. Axial CT image shows a large mass containing fat (arrow) and soft-tissue (arrowhead) components in the right side of the retroperitoneum. The duodenum, IVC, and aorta have been displaced by the tumor.



Figure 10. Desmoid tumor in a 34-year-old woman. Axial contrast-enhanced CT image shows a large heterogeneously enhancing mass (arrow) in the left side of the retroperitoneum below the spleen.

hemorrhage, compared with myelolipomas. Technetium 99m (^{99m}Tc) sulfur colloid scintigraphy can be used to confirm the presence of erythroid elements in myelolipomas (23).

Desmoid Tumor.—Fibromatosis is a group of conditions that arise from musculoaponeurotic structures and are characterized by fibrous soft-tissue proliferation that disrupts adjacent muscular and soft-tissue planes. Fibromatosis can be either superficial or deep. Desmoid tumor (deep

fibromatosis, aggressive fibromatosis, well-differentiated fibrosarcoma) is one of the forms of deep fibromatosis that constitutes 1.5%–3% of all soft-tissue masses (24) and accounts for less than 1% of retroperitoneal tumors. Desmoid tumor can be sporadic or associated with familial polyposis coli and Gardner syndrome. Desmoid tumor is hormonally responsive and dependent on estrogen. This tumor is more common in females, from puberty to 40 years, with a peak in occurrence in the 3rd decade (25,26). Histologically, desmoid tumor is composed of well-differentiated elongated uniform spindle cells, which are separated by collagen.

The imaging appearance of a desmoid tumor depends on the tissue composition (spindle cells, collagen, myxoid matrix) and the vascularity and may change with time. CT images show an ill- or well-defined mass with relatively high attenuation (Fig 10). At MR imaging, early-stage lesions are cellular and have high signal intensity on T2-weighted images; but with loss of cellularity and deposition of collagen, the lesion becomes hypointense on T2-weighted images. Hypointense tracks may also be seen that are due to dense collagen bands. Moderate to marked contrast enhancement is demonstrated on contrast-enhanced images. Deep desmoid tumor grows rapidly, is more aggressive, and is prone to recur (50%), even after wide surgical excision. Few cases of spontaneous regression and malignant transformation have been reported (27).

Miscellaneous Uncommon Neoplasms.—Chordoma is a tumor that arises from notochordal remnants and is seen most commonly in the sacrococcygeal region as a heterogeneously enhancing soft-tissue mass, with bone destruction of the sacrum and involvement of adjacent organs. Local recurrence is common.

Hemangiopericytoma is a vascular tumor that is lobulated, with speckled calcification. This tumor shows peripheral contrast enhancement.

Neurogenic Tumors

Neurogenic tumors constitute 10%–20% of primary retroperitoneal tumors (1). Compared with the mesenchymal tumors, neurogenic tumors occur in a younger age group and are more likely to be benign and have a better prognosis.

Neurogenic tumors can originate from the nerve sheath (schwannoma, neurofibroma, neurofibromatosis, malignant nerve sheath tumors), ganglionic cells (ganglioneuroma, ganglioneuroblastoma, neuroblastoma), or paraganglionic cells (paraganglioma, pheochromocytoma).

Neurogenic tumors are seen commonly (a) along the sympathetic ganglia, which are located in the paraspinal region, and (b) in the adrenal medulla or the organs of Zuckerkandl (paraortic bodies). Less commonly, neurogenic tumors occur in other sites, such as the urinary bladder, abdominal wall, bowel wall, or gallbladder (28).

Schwannoma.—Schwannoma, or neurilemoma, is a benign tumor that arises from the perineural sheath of Schwann (neurilemma). Schwannoma accounts for 6% of retroperitoneal neoplasms and is more common than neurofibroma. Schwannoma is usually asymptomatic and is more common in females (2:1), particularly in the 20–50-year age group (28). Pathologically, schwannoma is encapsulated and extends along the course of a nerve, with the nerve of origin flattened against the periphery of the tumor. Microscopically, the tumor is composed of alternating Antoni A and Antoni B areas. Antoni A areas are highly cellular, and Antoni B areas are less cellular, with cystic areas. Tumors with degenerative changes (ancient schwannomas) have hemorrhage, cystic changes, calcification, and hyalinization. In the retroperitoneum, schwannoma is commonly located in the paravertebral region and, less commonly, adjacent to the kidney, presacral space, and abdominal wall.

At CT, small schwannomas are round, well defined, and homogeneous, but large schwannomas may be heterogeneous in appearance. Calcification can be punctate, mottled, or curvilinear (Fig 11). The nerve of origin is often difficult to identify. After contrast enhancement, schwannoma demonstrates variable homogeneous or heterogeneous enhancement (28). At MR imaging, cellular areas are hypointense on T1- and T2-weighted images. Cystic areas appear hyperintense on T2-weighted images. Contrast enhancement is heterogeneous, with nonenhancing cystic components and enhancing solid components. Malignant transformation is rare (3,28,29).

Neurofibroma.—Neurofibroma is a benign nerve sheath tumor that can occur as an isolated tumor



Figure 11. Schwannoma in a 41-year-old woman. Axial CT image of the upper part of the abdomen shows an iso- to hypoattenuating mass in the left paravertebral region, with fine specks of calcification (arrowhead). The histopathologic findings from biopsy showed schwannoma.



Figure 12. Neurofibroma in a 37-year-old man. Axial CT image shows multiple well-defined homogeneous hypoattenuating neurofibromas (arrow) in a patient with type 1 neurofibromatosis.

(90%) or as part of type 1 neurofibromatosis. Approximately 30% of solitary tumors and 100% of multiple tumors or plexiform neurofibromas are associated with type 1 neurofibromatosis. Neurofibroma is more common in men, particularly in the 20–40-year age group (28). Histopathologically, neurofibroma is an unencapsulated solid



Figure 13. Plexiform neurofibroma in a 45-year-old woman with type 1 neurofibromatosis. Axial CT image shows an infiltrative hypoattenuating mass (arrow) encasing the celiac artery, portal vein, and IVC, with anterior displacement of the pancreas. Note also the mass (arrowhead) in the posterior pararenal space, posterior to the right kidney.

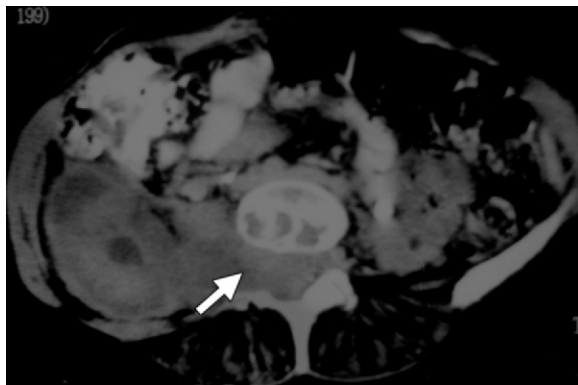


Figure 14. Neurofibrosarcoma in a 48-year-old man. Axial contrast-enhanced CT image obtained at the level of the L5 vertebra shows a large mass with areas of necrosis in the right posterior pararenal and paravertebral spaces. The mass extends into and expands the right intervertebral foramen (arrow) at the L4-L5 level.

tumor that (a) is composed of nerve sheath cells and collagen bundles with variable myxoid degeneration and (b) causes expansion of the entire nerve, with nerve fibers traversing the tumor. Cystic degeneration is rare.

At CT, neurofibroma is depicted as a well-defined round homogeneously hypoattenuating lesion (20–25 HU) because of the presence of lipid-rich Schwann cells and adipocytes and entrapment of adjacent fat (Fig 12). Typically, there

is homogeneous contrast enhancement (30–50 HU) that is due to collagen bands, but cystic areas caused by myxoid degeneration may be seen (28). Occasionally, targetlike enhancement can be seen. On T1-weighted images, the central portion of the tumor has higher signal intensity that is due to neural tissue, and on T2-weighted images, the periphery has higher signal intensity that is due to myxoid degeneration. Tumors involving the neural foramen have a dumbbell shape with expansion of the bone foramina or vertebral body scalloping. Plexiform neurofibroma is seen as a large extensive infiltrating mass (Fig 13). Malignant degeneration is more common with neurofibroma than with schwannoma, particularly in those patients who have neurofibromatosis (28).

Malignant Nerve Sheath Tumor.—Malignant nerve sheath tumors include malignant schwannoma, neurogenic sarcoma, and neurofibrosarcoma. Fifty percent of these tumors originate de novo, and the rest of them are derived from neurofibroma or ganglioneuroma or occur after exposure to radiation (28). Malignant nerve sheath tumors are more common in the 20–50-year age group, with no sex predilection. Progressive enlargement, pain, irregular margins, a heterogeneous nature, and infiltration into adjacent soft tissues are suggestive of malignancy (Fig 14), especially when associated with type 1 neurofibromatosis (1).

Ganglioneuroma.—Ganglioneuroma is a rare benign tumor that arises from the sympathetic ganglia. It is usually asymptomatic but can manifest with pain or a mass. Ganglioneuroma occasionally secretes hormones such as catecholamines, vasoactive intestinal peptides, or androgenic hormones (30). This tumor is commonly seen in the 20–40-year age group, with no sex predilection (28,31). Histopathologically, ganglioneuroma is composed of Schwann cells, ganglion cells, and nerve fibers. The retroperitoneum (32%–52% of cases) and mediastinum (39%–43% of cases) are the most common sites for ganglioneuroma, followed by the cervical region (8%–9% of cases). In the retroperitoneum, the tumor is commonly seen along the paravertebral sympathetic ganglia (59% of cases) or, less commonly, in the adrenal medulla.

At CT, ganglioneuroma is depicted as a well-circumscribed lobulated hypoattenuating mass that may surround a blood vessel without narrowing

the lumen. Discrete punctate calcifications are seen in 20%–30% of ganglioneuromas, unlike the coarse amorphous calcification of neuroblastomas (32). Necrosis and hemorrhage are uncommon, and contrast enhancement is variable. At MR imaging, ganglioneuroma is homogeneously hypointense on T1-weighted images, with varying signal intensity on T2-weighted images, depending on the myxoid, cellular, and collagen components. A whorled appearance at MR imaging has been reported that is due to interlacing bundles of longitudinal and transverse Schwann cells or to collagen fibers (Fig 15). Generally, ganglioneuroma is larger and has more calcification than a nerve sheath tumor. The prognosis is good after surgical resection of a ganglioneuroma (28).

Ganglioneuroblastoma and Neuroblastoma.—Ganglioneuroblastoma is an intermediate-grade tumor that has elements of benign ganglioneuroma and malignant neuroblastoma. Ganglioneuroblastoma is a pediatric tumor occurring in the 2–4-year age group, with no sex predilection, and is rare in adults. Imaging appearances vary, and the tumor could be solid or cystic with solid components.

Neuroblastoma is malignant and is more commonly seen in males and in the 1st decade of life. Two-thirds of neuroblastomas are located in the adrenal gland, and the remaining neuroblastomas occur along the paravertebral sympathetic chain. At CT and MR imaging, neuroblastoma is irregular, lobulated, and heterogeneous and demonstrates coarse amorphous calcifications and variable contrast enhancement, as well as invasion of adjacent organs and encasement of vessels with luminal compression. As many as 70% of patients have metastatic disease at the time of diagnosis (28).

Paraganglioma (Extraadrenal Pheochromocytoma).—The paraganglionic system is composed of neural crest cells, which are found in the adrenal medulla, parasympathetic ganglia, and chemoreceptors. Tumors that arise from the chromaffin cells of the adrenal medulla are called *pheochromocytomas*, and those that arise in an extraadrenal location (10%) are referred to as *paragangliomas*. Forty percent of paragangliomas produce high catecholamine levels, which result in symptoms such as headache, palpitations, excessive sweating, and elevated urinary metanephrine or vanillylmandelic

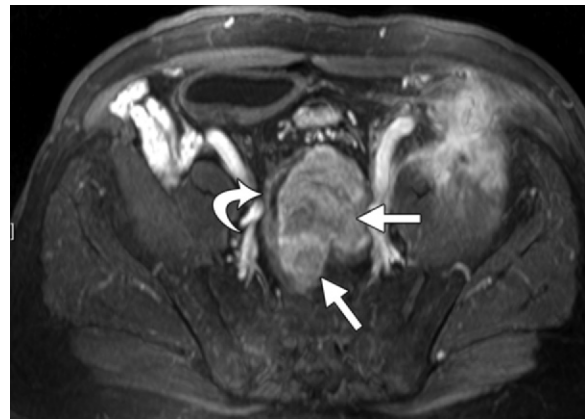


Figure 15. Ganglioneuroma in a 31-year-old man. Axial contrast-enhanced T1-weighted MR image shows a well-circumscribed lobulated mass with whorled enhancement (straight arrows) in the pelvic retroperitoneum. The mass is displacing the rectum (curved arrow) to the right side. The histopathologic findings from biopsy showed ganglioneuroma.

acid levels. Rarely, paraganglioma can manifest with acute abdomen caused by retroperitoneal hemorrhage. Paraganglioma can be associated with type 1 neurofibromatosis, multiple endocrine neoplasia syndrome, and von Hippel–Lindau syndrome. Paraganglioma is commonly seen in the 3rd to 4th decades, with no sex predilection. In the retroperitoneum, the most common site for a paraganglioma is the organs of Zuckerkandl, which are located anterior to the aorta at the level of the origin of the inferior mesenteric artery.

At CT, paraganglioma is usually seen as a large well-defined lobular tumor with areas of hemorrhage and necrosis. Punctate calcification is seen in 15% of cases, and a fluid-fluid level can be seen that is due to hemorrhage. Because of the hypervascular nature of paraganglioma, intense contrast enhancement is seen. Although there were earlier reports of hypertensive crisis with administration of intravenous contrast material, the findings in other studies have shown that low-osmolar nonionic contrast agents do not elevate serum catecholamine levels (33) and can be safely administered in patients with paragangliomas, even without administration of α -adrenergic blocking agents (34). At MR imaging, signal voids can be seen with T1-weighted spin-echo sequences. Variable signal intensity is seen on T2-weighted images. Although paraganglioma may be “bright” (Fig 16), the tumor is usually complex and heterogeneous (because of hemorrhage) (28) and almost never demonstrates “lightbulb”

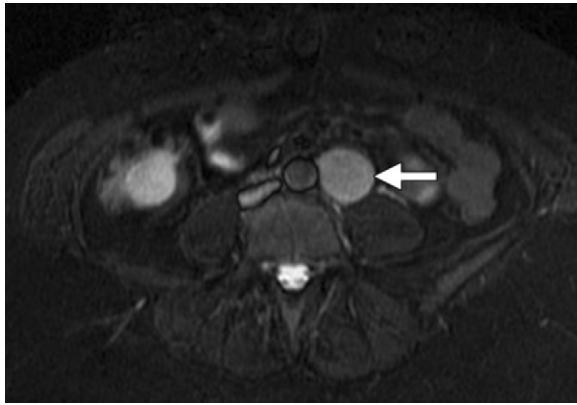


Figure 16. Paraganglioma in a 29-year-old man. Axial STIR MR image obtained at the level of the aortic bifurcation shows a well-defined hyperintense mass (arrow) lateral to the lower part of the abdominal aorta, a finding that is consistent with a paraganglioma in the organ of Zuckerkindl.

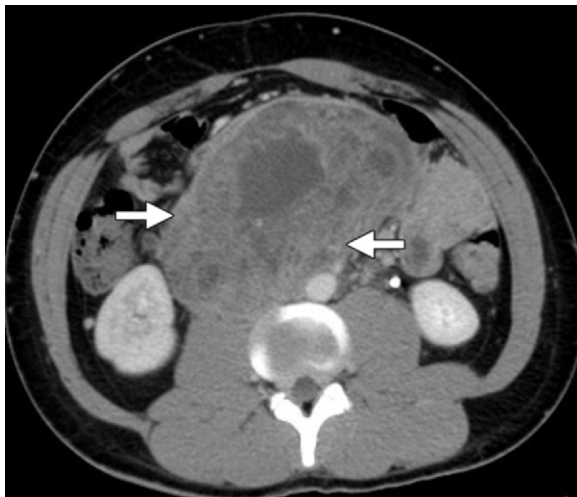


Figure 17. Primary nonseminomatous germ cell tumor in a 28-year-old man. Axial CT image shows a large heterogeneous mass (arrows) in the retroperitoneum. The histopathologic findings from biopsy showed that this mass was a primary retroperitoneal embryonal carcinoma.

high signal intensity with current imaging techniques (35). Radionuclide imaging performed after administration of *m*-iodobenzylguanidine (MIBG) shows high uptake in paragangliomas and is a sensitive technique for localizing these lesions (28). Paragangliomas are more aggressive tumors, with 22%–50% having metastases, compared with 2%–10% of adrenal pheochromocytomas. Rupture and retroperitoneal hemorrhage can also be seen in large paragangliomas (1).

Germ Cell, Sex Cord, and Stromal Cell Tumors

Primary Extragenadal Germ Cell Tumors.—Although germ cell tumors are seen most commonly in the testes or ovaries, 1%–2.5% of germ cell tumors originate in an extragenadal location. These tumors are believed to arise from aberrant primordial germ cell rests that are due to (a) faulty migration of germ cells from the yolk sac or endoderm to the urogenital ridge or (b) germ cells distributed physiologically to liver, bone marrow, and brain (36). Before a diagnosis of primary extragenadal germ cell tumor is made, a primary gonadal lesion should be excluded because retroperitoneal metastasis is seen in 30% of gonadal tumors. Occasionally the primary gonadal tumor might not be visible because tumor regression has left only a scar, with synchronous or asynchronous metastasis. Primary extragenadal germ cell tumor is more common in men. Histopathologically, these tumors can be seminomas or nonseminomatous germ cell tumors, which include embryonal carcinoma, yolk sac tumor, choriocarcinoma, teratoma, and mixed germ cell tumors. Elevated levels of α -fetoprotein (embryonal carcinoma, yolk sac tumors) and of the beta subunit of human chorionic gonadotropin (choriocarcinoma) may be found with laboratory tests. The retroperitoneum is the second most common site of extragenadal germ cell tumor after the mediastinum (36). Extragenadal germ cell tumor is often seen in or near the midline, especially between the T6 and S2 vertebrae. A midline mass is more suggestive of a primary extragenadal germ cell tumor than of metastasis.

At CT and MR imaging, the findings for primary extragenadal germ cell tumors are nonspecific. The imaging appearances are similar to those of gonadal germ cell tumors. Seminoma is rare in the retroperitoneum and is seen as a large, lobulated, well-defined homogeneous solid mass (37) with fibrous septa and ringlike or speckled calcification. At MR imaging, the septa are hypointense on T2-weighted images and show contrast enhancement. Nonseminomatous germ cell tumors are depicted as heterogeneous tumors with areas of hemorrhage, necrosis, and heterogeneous enhancement (Fig 17). Flow voids that are due to hypervascularity may be seen, as well as invasion of adjacent structures. The tumors in the extragenadal sites have a worse prognosis than that of their gonadal counterparts (37).

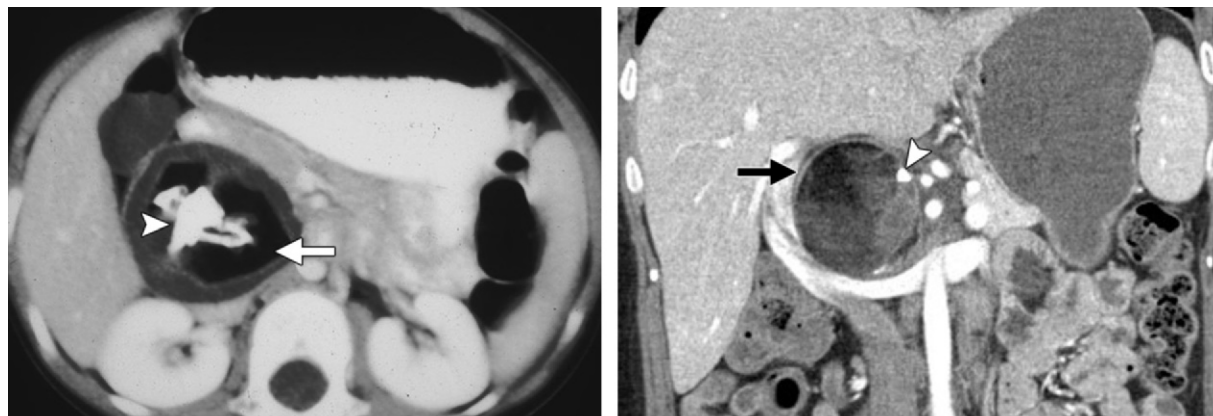


Figure 18. Mature teratoma. **(a)** Axial CT image of a 21-year-old woman with a mature teratoma shows a well-defined heterogeneous mass that demonstrates fat (arrow) and teeth (arrowhead). **(b)** Coronal CT image of a 26-year-old woman with a mature teratoma shows a well-defined round heterogeneous mass with fat attenuation (arrow). A focal area of calcification (arrowhead) is also depicted. The portal vein and IVC have been displaced without compression by the tumor.

Teratoma.—Teratoma is a germ cell tumor that originates from pluripotent germ cells that have been interrupted in their normal migration to the genital ridges. Less than 10% of teratomas are found in the retroperitoneum. Teratoma accounts for as many as 11% of primary retroperitoneal tumors and is the third most common tumor in the retroperitoneum in children, after neuroblastoma and Wilms tumor (38). Teratoma is more common in females, with a bimodal age distribution (<6 months and early adulthood). Teratoma can be benign or malignant, and benign teratoma can be either mature or immature.

Mature teratoma (dermoid cyst) contains well-differentiated tissues from at least two germ cell layers. Ectodermal layers are seen in all, mesodermal layers in 90% of lesions, and endodermal layers in the majority of lesions. Mature teratomas are predominantly cystic. Calcification (toothlike or well defined) and fat can be seen in 56% and 93% of cases, respectively (37) (Fig 18). **A fat-fluid (sebum) level and chemical shift between fat and fluid are pathognomonic.** A villiform solid component known as a Rokitansky protuberance is seen in 81% of cases. Malignancy has been reported in 2%–3% of mature teratomas, more commonly in children (26%) than adults (10%), and is associated with wall thickening, irregular margins, and infiltration of adjacent organs.

Teaching Point

Compared with mature teratoma, immature teratoma is less common (<1%), contains more than 10% undifferentiated tissue, and is seen in a younger age group (<20 years). The most common location of immature teratoma is near the upper pole of the left kidney (37). Immature teratoma is predominantly solid, with scattered areas of fat and calcification (coarse and ill defined), but cystic components are found occasionally.

Malignant teratoma can have germ cell or non-germ cell malignant tissue. Malignant transformation is less common in the retroperitoneum (38). Malignant tumors are irregular, with invasion of adjacent structures and vascular invasion. A poor prognosis is associated with lesions with germ cells or lesions with rhabdomyosarcoma or neural differentiation. An elevated α -fetoprotein level is found in 50% of malignant teratomas. Surgical resection is required for definitive diagnosis and treatment.

Primary Sex Cord Stromal Tumors.—Extraovarian primary sex cord stromal tumor arises from ectopic sex cord stromal tissue or from sex cord-like differentiation of somatic cells. This tumor is extremely rare and is seen in women, with a wide age distribution (30–76 years) (39). Extraovarian primary sex cord stromal tumor is more commonly seen in the pelvis along the broad ligament or fallopian tubes and is less commonly seen in the retroperitoneum or adrenal glands. Most of these



Figure 19. Granulosa cell tumor in a 44-year-old woman. Axial CT image shows a large heterogeneous mass with areas of curvilinear calcification (arrow) in the retroperitoneum.



Figure 20. Lymphoma in a 27-year-old woman. Axial contrast-enhanced CT image shows a large lobulated irregular homogeneous mass (straight arrows) that is encasing and anteriorly displacing the abdominal aorta (curved arrow). This displacement produces the characteristic floating aorta sign or CT angiogram sign.

tumors are granulosa cell tumors (Fig 19). Thecomas, Sertoli-Leydig cell tumors, and other unclassified sex cord tumors are rare. An elevated estrogen level may be seen in granulosa cell tumors and thecomas (39). Hormone-related symptoms such as amenorrhea and abnormal bleeding can be seen. The imaging findings are nonspecific. CT and MR images show heterogeneous solid tumors, with heterogeneous enhancement (40).

Lymphoid and Hematologic Neoplasms

Lymphoma.—Lymphoma is the most common retroperitoneal malignancy, accounting for 33% of all of these cases (1). Lymphoma can be broadly divided into Hodgkin lymphoma and non-Hodgkin lymphoma. Hodgkin lymphoma has a bimodal age distribution, occurring in patients in their 20s and 60s, and manifests with limited disease, often involving the mediastinum and spleen. Non-Hodgkin lymphoma is seen in the 40–70-year age group and frequently manifests with extranodal disease in the liver, spleen, or bowel, often at an advanced stage. Para-aortic lymph nodes are involved in 25% of the patients with Hodgkin lymphoma and 55% of the patients with non-Hodgkin lymphoma. Approximately 14% of the patients with non-Hodgkin lymphoma present with a retroperitoneal mass. Mesenteric lymph nodes are also more commonly involved in non-Hodgkin lymphoma.

At CT, lymphoma is seen as a well-defined homogeneous mass, with mild homogeneous contrast enhancement, that spreads between normal structures without compressing them. The aorta and IVC can be anteriorly displaced, producing the “floating aorta” or “CT angiogram” sign (Fig 20). Calcification and necrosis are unusual before therapy. At MR imaging, lymphoma is usually isointense on T1-weighted images and iso- to hyperintense on T2-weighted images, with moderate homogeneous or patchy enhancement after contrast material administration (41). Twenty-three percent of non-Hodgkin lymphomas are heterogeneous, and they cannot be distinguished from other primary retroperitoneal tumors on the basis of their enhancement characteristics alone (1). Obstruction of the ureters and IVC may be found.

Lymphoma is treated with chemotherapy or radiation therapy. Soft-tissue masses persist after treatment because of fibrosis and cannot be differentiated from viable tumor. Fibrosis has low signal intensity on T2-weighted MR images, with minimal enhancement. Positron emission tomography (PET) shows a high uptake of fluorine 18 fluorodeoxyglucose (FDG) in viable tumor, but there is no uptake in fibrosis.

Posttransplant Lymphoproliferative Disease.—

Posttransplant lymphoproliferative disease is a polyclonal or monoclonal proliferation of B lymphocytes that occurs as a complication of solid organ transplantation and immunosuppression. The disease is seen in 2%–8.4% of patients who have undergone liver transplantation, with a mean delay in appearance of 7–14 months. Most (80%) of these cases are associated with Epstein-Barr virus infection, and the manifestations range from benign infectious mononucleosis to non-Hodgkin lymphomas. Imaging features include lymphadenopathy, splenomegaly, masses in the liver or kidney, and bowel lesions. Extensive retroperitoneal lymphadenopathy may be found (42) (Fig 21).

Extramedullary Plasmacytoma.—Extramedullary plasmacytoma is a rare plasma cell neoplasm (3%–4%) that is characterized by monoclonal proliferation of plasma cells. Clinical symptoms depend on the organs affected. Extramedullary plasmacytoma is more common in males, with a peak incidence in the 6th and 7th decades. The diagnosis is made only after excluding multiple myeloma in the bone marrow or any bone lesion by using a skeletal survey or bone marrow MR imaging, with normal results of plasma electrophoresis. Although extramedullary plasmacytoma is most common in the aerodigestive tract (80%), it can be found in almost any organ. In the retroperitoneum, extramedullary plasmacytoma is seen most commonly in the perirenal region because of the activity of primitive angiohematopoietic stem cells. CT and MR imaging show a focal or extensive infiltrating soft-tissue mass, with homogeneous contrast enhancement (Fig 22). Extrasosseous plasmacytoma has a better prognosis than the solitary bone plasmacytoma. Plasmacytoma progresses to myeloma in 50% of cases (43,44).

Solid Nonneoplastic Masses**Lipomatosis**

Lipomatosis is a benign metaplastic overgrowth of mature unencapsulated white fat. Lipomatosis may be asymptomatic or associated with nonspecific symptoms, including lower abdominal pain and urinary or gastrointestinal symptoms. Lipomatosis is more common in males (18:1), particularly African Americans, with a mean age of 48 years, and is not associated with obesity.



Figure 21. Posttransplant lymphoproliferative disease in a 59-year-old man with a history of liver transplantation. Axial CT image shows a large infiltrative soft-tissue mass (arrow) in the retroperitoneum. The mass encases and anteriorly displaces the aorta and the IVC.

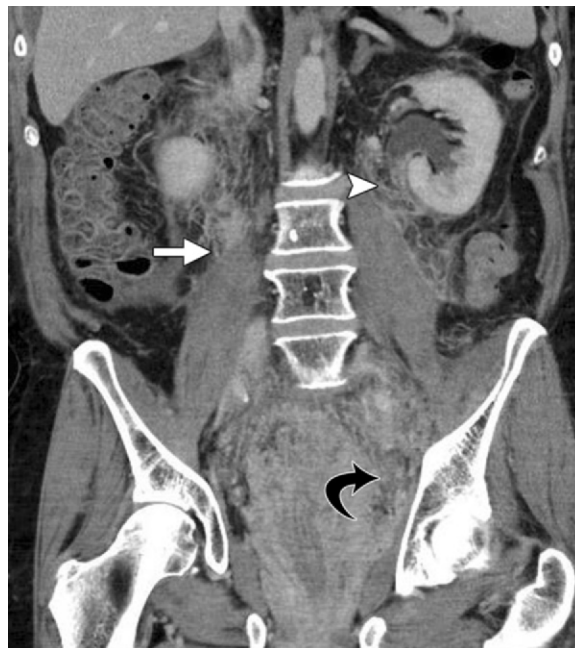


Figure 22. Extramedullary plasmacytoma in a 68-year-old man. Coronal contrast-enhanced CT image shows enhancing soft-tissue masses in the abdominal (straight arrow), perirenal (arrowhead), and pelvic (curved arrow) retroperitoneal spaces.

Histopathologically, lipomatosis is composed of homogeneous, mature, adult white fat cells separated by fibrous septa. Lipomatosis is seen commonly in the pelvis and along the perirectal and perivesicular spaces and is seen less commonly

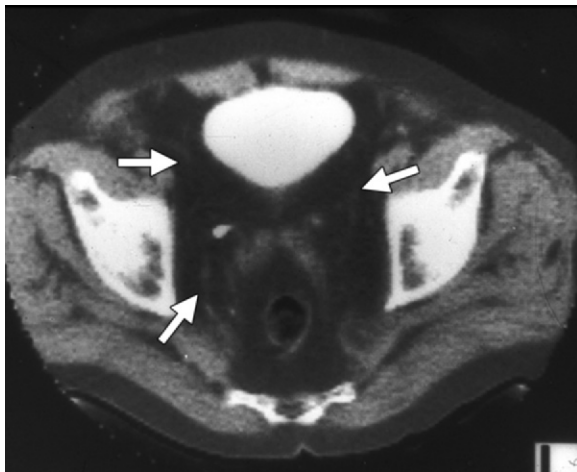


Figure 23. Pseudotumoral lipomatosis in a 47-year-old man. Axial CT image shows extensive fat proliferation (arrows) in the pelvic retroperitoneal space. The fat is compressing and anteriorly displacing the bladder.



Figure 24. Active retroperitoneal fibrosis in a 49-year-old man. Axial contrast-enhanced CT image shows a well-defined enhancing rind of soft tissue (arrow) surrounding the abdominal aorta.

in the abdominal retroperitoneum. CT and MR imaging show excess fat in the pelvis crowding the anatomic structures, with a few fibrous tissue strands but no soft-tissue mass or enhancement (Fig 23). A pear-shaped bladder is produced by symmetric compression and displacement of the bladder caused by pelvic lipomatosis. The lower portions of the ureters may be pinched medially, with resultant hydroureteronephrosis. The femoral veins may be stretched. Patients with severe urinary obstruction may require ureteral stents, urinary diversion, and fat excision (12).

Retroperitoneal Fibrosis

Retroperitoneal fibrosis is an uncommon collagen vascular disease of unknown cause that can mimic a retroperitoneal tumor. Retroperitoneal fibrosis is typically idiopathic (>70% of cases) and is likely autoimmune in origin. It has also been postulated that retroperitoneal fibrosis is an exaggerated inflammatory response to ceroid produced in atherosclerotic plaques. Retroperitoneal fibrosis can be secondary to drugs, malignancy, hemorrhage, inflammatory conditions, infection, radiation, chemotherapy, renal trauma, and amyloidosis. Although retroperitoneal fibrosis manifests as an isolated retroperitoneal disease, it can also be associated with other fibrosing conditions, such as sclerosing cholangitis, Riedel thyroiditis, fibrotic pseudotumor of the orbit, and autoimmune pancreatitis, all of which form part of the group labeled “multifocal fibrosclerosis.” Retroperitoneal fibrosis can be asymptomatic in the early stages, but pain, extremity swelling, decreased urinary output, testicular swelling, and endometriosis may be seen in the chronic stage. Retroperitoneal fibrosis is more common in males (3:1), particularly in the 40–60-year age group. Histopathologically, retroperitoneal fibrosis is characterized by ill-defined plaque-like fibrous proliferation around the aorta, iliac arteries, IVC, and ureters. The disease progresses from chronic active inflammation to fibrous scarring (45). **Retroperitoneal fibrosis is seen most commonly surrounding the infrarenal abdominal aorta and proximal common iliac arteries.**

CT shows an irregular plaque-like soft-tissue mass in the retroperitoneum, located around the aortic bifurcation and extending along the iliac arteries and involving the ureters, duodenum, pancreas, and spleen. Retroperitoneal fibrosis does not displace the aorta and IVC anteriorly, as lymphoma or metastatic nodes often do, but causes tethering of these structures to the underlying vertebrae. Avid enhancement is seen in the active stages of retroperitoneal fibrosis (Fig 24), with little or no enhancement in the chronic phase. MR imaging shows high signal intensity on T2-weighted images in the acute phase of the disease, with early contrast enhancement, and shows low signal intensity in the chronic fibrosing phase (Fig 25), with delayed enhancement. Associated features that are suggestive of retroperitoneal fibrosis are abdominal aortic

Teaching
Point

aneurysms, history of radiation exposure, methysergide ingestion, and medial displacement of the ureters (1). Gallium 67 scans show high uptake in the active stages of the disease and little or no uptake in the chronic fibrotic stage. The FDG PET scan shows increased uptake of FDG and is useful for detecting metabolic activity and distant disease (45). Malignant retroperitoneal fibrosis is produced when small retroperitoneal neoplastic foci elicit a desmoplastic response, and malignant retroperitoneal fibrosis may be difficult to distinguish from nonmalignant retroperitoneal fibrosis. Compared with nonmalignant retroperitoneal fibrosis, malignant retroperitoneal fibrosis is larger, with irregular lobular nodular margins, is located more cephalad, and shows mass effect, displacing the aorta and IVC anteriorly and the ureters laterally, with variable contrast enhancement. Imaging-guided biopsy may be required for confirmation of the diagnosis. Treatment is with steroids, immunotherapeutic drugs, disease-modifying antirheumatic drugs, tamoxifen, or surgery (46).

Erdheim-Chester Disease

Erdheim-Chester disease (lipoid granulomatosis or polyostotic sclerosing histiocytosis) is a rare non-Langerhans form of histiocytosis of unknown origin, with distinct microscopic, immunohistochemical, clinical, and radiologic features (47,48). The clinical spectrum ranges from asymptomatic bone lesions to systemic illness and death. Bone pain, exophthalmos, diabetes insipidus, fever, weight loss, and malaise can also be found. Erdheim-Chester disease has a wide age distribution, with no sex predilection (48). Histologically, there is xanthogranulomatous infiltration with foamy histiocytes surrounded by fibrosis, without Birbeck granules or S-100 immunostaining. Extraskelatal lesions are seen in 50% of cases of Erdheim-Chester disease, with retroperitoneal involvement seen in one-third (45). Radiography shows characteristic bilateral symmetric osteosclerosis of the metaphyseal-diaphyseal region of the long bones, with sparing of the epiphysis and lesser involvement of the flat bones and axial skeleton. Retroperitoneal involvement with Erdheim-Chester disease characteristically produces a soft-tissue rind of fibrous perinephritis surrounding the kidneys and ureters, which can result in renal failure (Fig 26). MR imaging shows low signal intensity on T1- and T2-weighted images, with minimal contrast

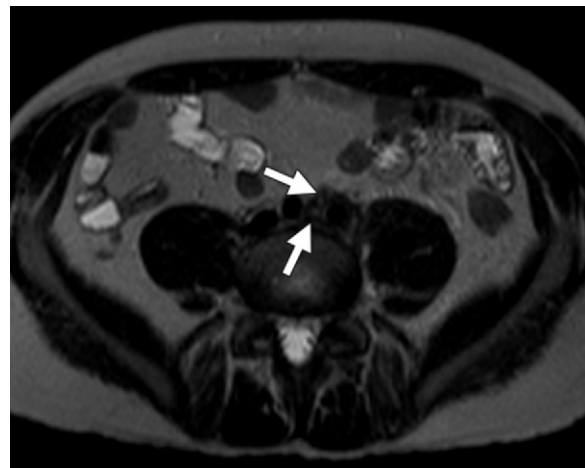


Figure 25. Chronic retroperitoneal fibrosis in a 55-year-old woman. Axial T2-weighted spin-echo MR image obtained at the level of the aortic bifurcation shows a hypointense rind of chronic retroperitoneal fibrosis (arrows) encasing the lower part of the aorta. There is no aortic aneurysm.



Figure 26. Erdheim-Chester disease in a 26-year-old man. Axial CT image obtained at the level of the kidneys shows bilateral perirenal fibrosis (arrows).

enhancement (47). Treatment is with ureteral stents, steroids, chemotherapy, immunotherapy, radiation therapy, or surgery.

Extramedullary Hematopoiesis

Extramedullary hematopoiesis is characterized by abnormal deposits of hematopoietic tissue outside the bone marrow as a compensatory mechanism for reduced hematopoiesis by the bone marrow. Extramedullary hematopoiesis is seen in hemoglobinopathies, myelofibrosis, leukemia, lymphoma, and carcinomas. Clinically, the patient presents with organomegaly or vague abdominal symptoms. Histologically, erythroid precursors are seen in extramedullary sites. Extramedullary hematopoiesis can be seen in any



Figure 27. Extramedullary hematopoiesis in a 38-year-old man with thalassemia. Axial contrast-enhanced CT image of the pelvis shows an enhancing mass (arrow) in the presacral region.



Figure 28. Cystic lymphangioma in a 23-year-old woman. Axial CT image shows a homogeneous well-defined lobulated cystic mass (arrow) in the retroperitoneum. The mass displaces the IVC anteriorly and extends slightly across the midline.

organ of mesenchymal origin, although it is more common in the liver, spleen, and lymph nodes (49). Less commonly, extramedullary hematopoiesis affects the kidneys, mesentery, and pelvis. The retroperitoneum is an uncommon site. The typical CT appearance is hyper- or isoattenuating round or lobulated masses in the paravertebral region, with or without macroscopic fat (Fig 27). The MR imaging appearance is variable. Low signal intensity can be seen on T1- and T2-weighted images because of the red marrow or hemosiderin content. High signal intensity may be found on T1- and T2-weighted images because of fatty tissue. Enhancement is variable and often mild,

and there is no associated bone destruction or calcification. Secondary signs of chronic anemia, such as skeletal changes, an expanded diploic space, and signs of hemochromatosis can be seen. The diagnosis is evident when the patient has a known hemoglobinopathy and when characteristic skeletal changes are found (50).

Cystic Neoplastic Masses

Retroperitoneal cysts are uncommon. These cysts are usually asymptomatic but may produce symptoms that depend on the location, size, and complications. Retroperitoneal cysts should be differentiated from mesenteric, omental, splenic, and enteric duplication cysts.

Cystic Change in Solid Neoplasms

Cystic changes may develop in solid lesions such as paragangliomas and neurilemmomas. These are typically seen in the paravertebral region. Leiomyosarcoma can have extensive areas of necrosis (Fig 3) and may be predominantly cystic. Other sarcomas can also appear cystic after chemotherapy because of tumor necrosis and hemorrhage (51).

Cystic Teratoma

Cystic teratoma is a germ cell tumor that arises from differentiation of at least two germ cell layers. It is usually asymptomatic and is more common in females, particularly in newborn children. CT shows a complex cystic mass, with areas of fat and calcification. Unlike a solid teratoma, a cystic teratoma is usually benign.

Lymphangioma

Lymphangioma is a developmental malformation that is caused by failure of communication of retroperitoneal lymphatic tissue with the main lymphatic vessels. Lymphangioma accounts for 1% of all retroperitoneal neoplasms (3). It is usually asymptomatic and is more common in men (51). Lymphangioma can manifest in the first 2 years of life with abdominal distention or pain. Histopathologically, lymphangioma is characterized by thin-walled unilocular or multilocular cysts that are lined with a single endothelial layer and contain clear or milky fluid. Lymphangioma can be seen in perirenal, pararenal, or pelvic extraperitoneal spaces and can involve more than one compartment. CT shows a large thin-walled unilocular or multilocular cystic mass (Fig 28) with attenuation values ranging from that of fat (caused by chyle) to that of fluid. Calcification is rarely seen.

At MR imaging, lymphangioma has low signal intensity on T1-weighted images and high signal intensity on T2-weighted images. The MR imaging characteristics will also be altered by a large amount of chyle, with high signal intensity on T1-weighted images and intermediate signal intensity on T2-weighted images. An elongated shape and the involvement of multiple compartments are salient features of lymphangiomas, particularly those prone to recurrence. The occurrence of septa, compression of intestinal loops, and a lack of fluid in dependent recesses and mesenteric leaves differentiate lymphangioma from ascites. Treatment of lymphangioma involves complete excision, but recurrence is common (3,51).

Lymphangiomatosis

Lymphangiomatosis (cystic angiomatosis) is characterized by diffuse multisystemic lymphangiomas that are locally infiltrative, with growth along tissue planes (52–55). Histopathologically, these lymphangiomas are subdivided into simple, cavernous, and cystic subtypes and are commonly seen in the retroperitoneum and mesentery. At CT, the lymphangiomas appear as large well-defined nonenhancing cystic masses, which may have fine specks of calcification (Fig 29). Mesenteric thickening can be seen that is caused by dilated or obstructed lymphatic vessels. MR imaging is used to delineate the infiltrative components of tumor, which is helpful for surgical planning. Involvement of multiple organ systems is characteristic, obviating the need for biopsy. Chest involvement is more common in adults, with diffuse infiltration of the mediastinum, pleural thickening or effusion, septal thickening, and ground-glass opacities. In the bones, there are well-defined geographic lytic lesions with sclerotic borders that are caused by anomalous agenesis or insufficient lymphatic vessels. Whole-body short inversion time inversion-recovery (STIR) MR imaging is a sensitive method for the detection of bone lesions associated with this condition (56).

Lymphangioliomyoma

Lymphangioliomyoma is a retroperitoneal cystic mass that is produced because of lymphatic obstruction by proliferation of smooth muscle cells and the resultant dilated abdominal lymphatic vessels. Lymphangioliomyoma is the third most



Figure 29. Lymphangiomatosis in a 26-year-old man. Axial CT image shows a large multicystic mass with specks of calcification (arrowheads) in the retroperitoneum. The mass compresses the vascular structures and displaces the bowel loops. Lytic lesions (arrows) are depicted in the vertebra.



Figure 30. Lymphangioliomyoma in a 33-year-old woman. Axial CT image of the abdomen shows lobulated masses that contain cystic areas (arrows) in the superior retroperitoneal space.

common (16%–21% of these patients) abdominal manifestation of lymphangioliomyomatosis (57,58), after angiomyolipoma (70% of patients) and enlarged lymph nodes (57). Lymphangioliomyomatosis is a subtype of perivascular epithelioid cell tumor. Almost all of the patients with lymphangioliomyomatosis are female patients, and all have pulmonary cysts. A dilated thoracic duct and chylous ascites may also be seen. CT

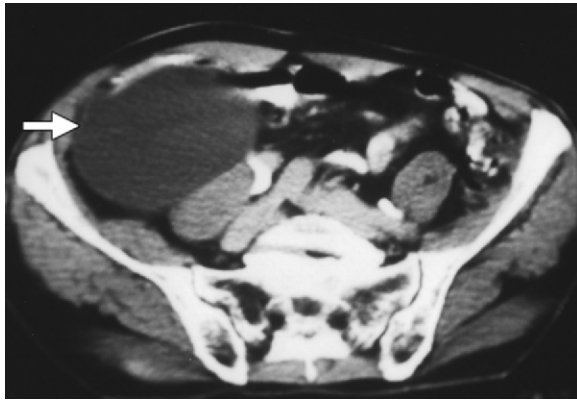


Figure 31. Mucinous cystadenoma of the retroperitoneum in a 39-year-old woman. Axial CT image of the abdomen shows that a nonspecific well-defined unilocular simple cyst (arrow) in the right retroperitoneal space is displacing the colon anteriorly.

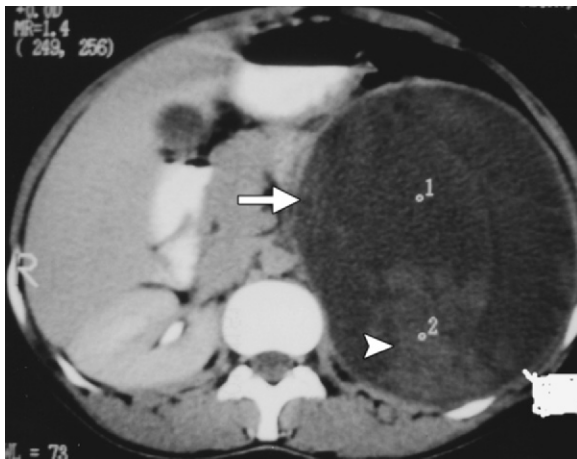


Figure 32. Serous cystadenocarcinoma in a 44-year-old woman. Axial contrast-enhanced CT image shows a large cystic mass (arrow), with solid papillary fronds (arrowhead) within it. The ovaries and pelvis were normal. 1, 2 = cursors used to measure attenuation values.

shows a cystic mass, which is homogeneously hypoattenuating, with attenuation values of 3–25 HU (Fig 30). At MR imaging, the mass is hypointense on T1-weighted images and hyperintense on T2-weighted images, with a well-defined wall. Typically, there is immediate peripheral enhancement after contrast material administration and homogeneous delayed (10-minute) enhancement in the center, likely caused by slow lymphatic flow into the cystic mass (58). Displacement of vascular structures is seen with large masses. Variations in the size of the mass have been reported with diet,

time of the day, and gravitational factors (59). In patients with lymphangiomyomatosis, a retroperitoneal cystic mass is assumed to be a lymphangiomyoma unless there are clinical indications of abscess or tumor (59).

Mucinous Cystadenoma or Cystadenocarcinoma

Mucinous cystadenoma is a rare primary epithelial retroperitoneal tumor that is believed to arise (a) secondary to invagination of peritoneal mesothelium with subsequent mucinous metaplasia and cyst formation, (b) as a result of ectopic ovarian tissue, (c) from a teratoma with single mucinous cell lineage, or (d) from remnants of the embryonic urogenital apparatus. Mucinous cystadenoma is asymptomatic and is seen in women with normal ovaries. Histologically, mucinous cystadenoma has a single layer of tall columnar epithelial cells. CT and MR imaging show a well-defined unilocular homogeneous cystic mass (Fig 31). This cyst requires surgical resection because of the risk of malignant transformation (60).

Serous Cystadenocarcinoma

Serous cystadenocarcinoma is an extremely rare primary epithelial retroperitoneal tumor that likely develops through serous or mucinous metaplasia of retroperitoneal coelomic mesothelium, which is deposited along routes of ovarian descent (61). Other theories of development include a teratoma, a supernumerary ovary, and an enterogenous cyst. Serous cystadenocarcinoma is seen in women with normal ovaries. Histopathologically, the tumor is encapsulated and multicystic, filled with serous fluid and protruding papillary nodules. CT and MR imaging findings are nonspecific and show a well-defined cystic lesion with solid intramural nodules, without any evidence of a primary ovarian mass. Enhancement of the wall and solid components may be found (Fig 32). Other findings include (a) an elevated carcinoembryonic antigen level in the serum and (b) glandular epithelial cells at biopsy (61). This cyst requires surgical excision with wide clearance margins. Other less common primary retroperitoneal epithelial neoplasms include borderline mucinous tumor, mucinous cystadenocarcinoma, and borderline serous tumor.

Cystic Mesothelioma

Cystic mesothelioma is a benign neoplasm of the serosal lining of the peritoneal space. Cystic mesothelioma has no causal relationship to asbestos exposure, manifests with abdominal pain, and is more common in females. Histopathologically, cystic mesothelioma is a unilocular or multilocular thin-walled cyst with watery contents. Cystic mesothelioma is uncommon in the retroperitoneum. CT and MR imaging show a multilocular thin-walled cystic lesion, which is indistinguishable from other cystic lesions. Local recurrence may be seen (56).

Müllerian Cyst

Müllerian cyst is a rare benign urogenital cyst that arises from aberrant müllerian duct remnants in the retroperitoneum. This cyst proliferates with abnormal hormonal stimulation, such as in obese women with menstrual irregularities. A müllerian cyst can be the pronephric, mesonephric, or metanephric type. Histopathologically, the cyst has a smooth muscle wall that is lined internally with cuboidal or columnar epithelial cells. At CT and MR imaging, a unilocular or multilocular cyst with thin walls containing clear fluid is depicted. The clinical features enable differentiation from other cystic neoplasms (56).

Epidermoid Cyst

Epidermoid cyst is a congenital ectodermal cyst that is caused by desquamation of epithelial cells. The cyst is asymptomatic or produces pressure symptoms such as constipation or lower abdominal pain. Epidermoid cyst is more common in women. Histopathologically, the cyst is lined with stratified squamous epithelium and contains desquamated debris, keratin, cholesterol, and water. Epidermoid cyst is most commonly seen in the presacral space. CT and MR imaging show a unilocular thin-walled cyst in the presacral space (56).

Tailgut Cyst

Tailgut cyst originates from embryonic hindgut remnants. This cyst is usually asymptomatic and is more common in middle-aged women. Histologically, tailgut cyst is lined with various types of epithelium. Tailgut cyst is most commonly seen in the presacral space, between the rectum and sacrum. CT and MR imaging depict a well-defined multilocular mass in the presacral space that demonstrates attenuation values ranging

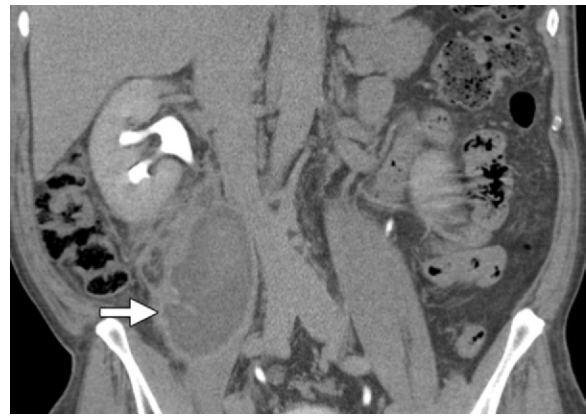


Figure 33. Retroperitoneal hematoma in a 51-year-old man who had undergone bone marrow biopsy. Coronal CT image obtained after the biopsy shows a heterogeneous predominantly cystic-appearing hematoma (arrow) in the right retroperitoneal space. The mass is displacing the IVC.

from that of water to that of soft tissue and shows occasional calcification. Surgical resection is required because of the risk of malignant degeneration, which manifests at CT with involvement of adjacent structures and loss of discrete margins.

Cystic Nonneoplastic Masses

Hematoma

Retroperitoneal hematoma is caused by trauma, blood dyscrasia, anticoagulation therapy, rupture of an abdominal aortic aneurysm, or interventional or surgical procedures. Retroperitoneal hematoma can have a variable imaging appearance, depending on its stage. Acute and subacute hematomas have heterogeneous high attenuation at CT and may be hyperintense on T1- and T2-weighted images. Chronic hematomas have low attenuation on CT images (Fig 33) and low signal intensity on MR images because of hemosiderin deposition. Occasionally, the heterogeneous appearance on contrast-enhanced CT images can be confused with a sarcoma, but the well-defined margin, the absence of contrast enhancement, and the changing appearance with time, with a progressive decrease in size, distinguish retroperitoneal hematoma from sarcoma (45,56).

Urinoma

Urinoma is a collection of extravasated urine that is found secondary to trauma or iatrogenic causes. A well-defined cystic lesion is seen in the retroperitoneum, more commonly in the peri-

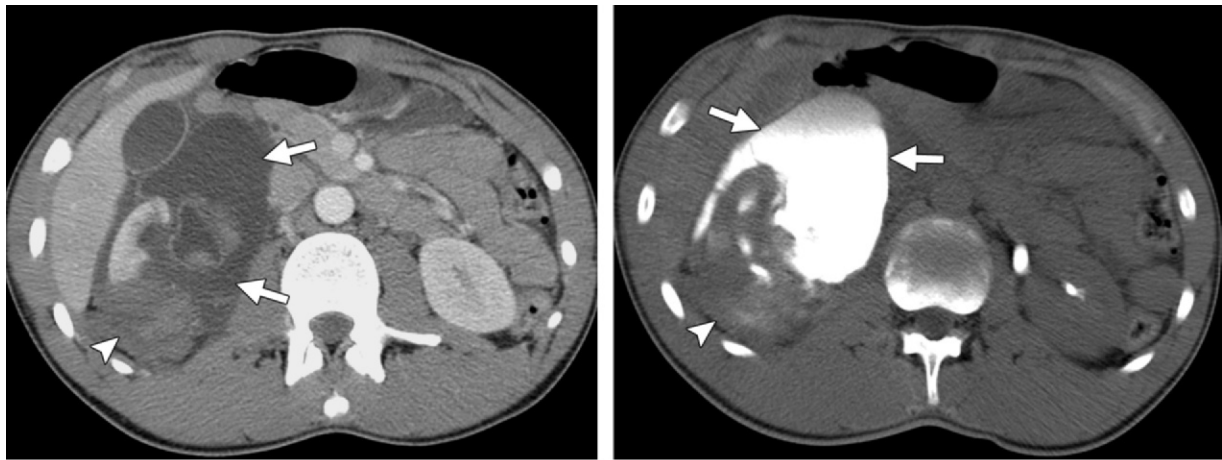


Figure 34. Urinoma in a 42-year-old man who had been in a motor vehicle accident. **(a)** Axial contrast-enhanced CT image obtained after the accident shows renal injury, with a hematoma (arrowhead) posteriorly and a large fluid collection (arrows) in the right anterior pararenal space. **(b)** Delayed axial contrast-enhanced CT image again shows the hematoma (arrowhead) and now shows the fluid collection filling with contrast material (arrows) excreted from the kidneys, a finding that indicates that this is a urinoma. (Images courtesy of Joel A. Gross, MD, Harborview Medical Center, Seattle, Wash.)



Figure 35. Lymphocele in a 43-year-old woman who had ovarian cancer and had undergone retroperitoneal lymphadenectomy. Axial CT image shows a large thin-walled unilocular cystic mass (straight arrow) in the right retroperitoneal space, a finding that is consistent with a lymphocele. Note the surgical clip (curved arrow) anterior to the right psoas major.

renal space. CT shows a well-defined fluid collection (Fig 34a), with progressively increasing attenuation caused by contrast-enhanced urine entering the urinoma (Fig 34b). Hydronephrosis is found in most of these patients (56).

Lymphocele

A lymphocele is a collection of lymph without an epithelial lining that is seen after retroperitoneal lymphadenectomy (in 12%–24% of these) or renal transplantation. A lymphocele may be asymptomatic or may manifest with lower limb edema (pressure effect on veins) or hydronephrosis (pressure on ureters). CT shows a homogeneous hypoattenuating mass (Fig 35). Negative attenu-

ation can be seen that is due to fat contained within the fluid. Calcification is rarely seen. The clinical history is helpful in the diagnosis (56).

Pancreatic Pseudocyst

Pancreatic pseudocyst is a collection of pancreatic fluid that occurs secondary to acute pancreatitis. Clinical features of acute or chronic pancreatitis are seen. Elevated serum and urine levels of amylase and lipase are found. Histopathologically, pancreatic pseudocyst is an encapsulated collection of pancreatic fluid, with an epithelial lining, and the fluid contains amylase. Pancreatic pseudocyst is seen commonly in the peripancreatic region but can be seen remote to the pancreas in the abdomen, pelvis, or mediastinum. CT shows a well-defined round or oval fluid collection with enhancing walls (Fig 36). Other features of acute pancreatitis may also be seen (56).

Nonpancreatic Pseudocyst

Nonpancreatic pseudocyst is rare and histopathologically is a collection of serous fluid, pus, or hemorrhage contained by a thick fibrous wall without an epithelial lining. Nonpancreatic pseudocyst is usually asymptomatic, without elevation of serum amylase or lipase levels. At CT, nonpancreatic pseudocyst is seen as a unilocular or multilocular fluid collection with thick walls (56).

Diagnostic Clues for a Retroperitoneal Mass

Although there is an overlap in the imaging appearances of retroperitoneal masses, the specific imaging features and patterns of involvement, when combined with clinical features and demographics, can be used to narrow the differential diagnosis (Table 3).

A pure fat-containing mass implies either a lipoma or a well-differentiated liposarcoma. Unlike lipoma, a well-differentiated liposarcoma has thicker, irregular, and nodular septa that show contrast enhancement. A heterogeneous mass containing fat could be a dedifferentiated liposarcoma, myelolipoma, or angiomyolipoma. Liposarcoma is usually larger and less well defined than a myelolipoma. ^{99m}Tc-sulfur colloid scintigraphy can be used to confirm the presence of erythroid elements in a myelolipoma. Enlarged vessels coursing through the mass, aneurysms, and associated hemorrhage are features that differentiate an angiomyolipoma from a liposarcoma. A fat-fluid level is typically seen in a teratoma but has also been described in a well-differentiated liposarcoma (38). A mass with fat and calcification or teeth is pathognomonic of teratoma.

Myxoid stroma has low signal intensity on T1-weighted MR images and high signal intensity on T2-weighted MR images, with delayed contrast enhancement. This type of stroma is more commonly seen in myxoid liposarcoma, neurogenic tumors, and myxoid malignant fibrous histiocytoma (3,4). Necrotic changes appear hypointensifying at CT and show low signal intensity on T1-weighted MR images and high signal intensity on T2-weighted MR images, without contrast enhancement. A large mass with extensive necrosis and invasion of the IVC is suggestive of a leiomyosarcoma.

Vascular tumors such as paragangliomas and hemangiopericytomas demonstrate flow voids on spin-echo T1-weighted MR images, hemorrhagic necrosis with fluid-fluid levels, and intense contrast enhancement. Myxoid malignant fibrous histiocytoma, leiomyosarcoma, and other sarco-



Figure 36. Pancreatic pseudocyst in a 37-year-old man with acute pancreatitis. Axial CT image shows edema (curved arrow) in the peripancreatic region and a unilocular cystic collection (straight arrow) in the left anterior pararenal space, a finding that is consistent with a pancreatic pseudocyst. Analysis of the fluid obtained at aspiration of the cyst revealed amylase in the cystic collection.

mas are moderately vascular; and lymphoma, low-grade liposarcoma, and benign tumors are generally hypovascular, without appreciable contrast enhancement. Densely cellular or fibrous masses have low signal intensity on T2-weighted images. These masses include neoplasms such as lymphoma, round cell tumors, and desmoid tumors, as well as nonneoplastic masses such as retroperitoneal fibrosis and Erdheim-Chester disease.

A paravertebral mass is more likely to be a neurogenic tumor and, when manifesting with hypertension and elevated catecholamine levels, is consistent with a paraganglioma. A tumor that spreads between normal structures and encases vessels without compressing them could be a lymphangioma, ganglioneuroma, or lymphoma. Paraganglioma and ganglioneuroma generally extend along the sympathetic chain. A mantle-like soft-tissue mass around the lower part of the aorta or IVC could be a lymphoma, retroperitoneal fibrosis, or Erdheim-Chester disease. Before treatment, lymphoma is typically homogeneous, with lobular irregular margins, and causes mass effect. Retroperitoneal fibrosis is associated with tethering of the ureters and IVC. Erdheim-Chester disease is associated with perinephric fibrosis and bone lesions. The floating aorta sign or CT angiogram sign is typically seen in lymphoma because of anterior displacement of the aorta and IVC by the mass. The differential diagnosis of a solid mass with calcification includes teratoma, malignant fibrous histiocytoma, chondrosarcoma, Ewing sarcoma, dedifferentiated liposarcoma, and synovial sarcoma.

Table 3
Imaging Features Suggestive of a Specific Diagnosis for Retroperitoneal Masses

Imaging Feature	Diagnosis
Pure fat-containing mass	Lipoma, well-differentiated liposarcoma
Heterogeneous mass with fat	Dedifferentiated liposarcoma, myelolipoma, angiomyolipoma
Fat-fluid level	Teratoma, well-differentiated liposarcoma
Fat with calcification, teeth, or fluid	Teratoma
Myxoid stroma	Myxoid liposarcoma, neurogenic tumor, myxoid malignant fibrous histiocytoma (<i>less common diagnoses</i> : desmoid tumor, hemangiopericytoma, leiomyoma or leiomyosarcoma, rhabdomyosarcoma, malignant mesenchymoma)
Large mass, extensive necrosis, invasion of IVC	Leiomyosarcoma
Fluid-fluid level caused by hemorrhage	Paraganglioma
Extremely hypervascular	Paraganglioma, hemangiopericytoma
Moderately hypervascular	Myxoid malignant fibrous histiocytoma, leiomyosarcoma, other sarcoma
Hypovascular	Lymphoma, low-grade liposarcoma, benign tumor
T2 hypointensity	Lymphoma, desmoid tumor, small round cell tumor, retroperitoneal fibrosis, Erdheim-Chester disease
Paravertebral mass	Neurogenic tumor
Paravertebral mass, high catecholamine levels, hypertension	Paraganglioma
Extension between normal structures, encasement without luminal compression	Lymphangioma, ganglioneuroma, lymphoma (floating aorta or CT angiogram sign)
Extension along normal structures	Paraganglioma, ganglioneuroma
Mantlelike mass around aorta or IVC	Lymphoma, retroperitoneal fibrosis, Erdheim-Chester disease
Floating aorta or CT angiogram sign	Lymphoma
Soft-tissue mass with calcification	Malignant fibrous histiocytoma, teratoma, extraosseous chondrosarcoma/Ewing sarcoma, synovial sarcoma, dedifferentiated liposarcoma
Cystic mass with solid tumor enhancement	Myxoid liposarcoma, schwannoma, neurofibroma
Cystic mass with slow, progressive enhancement	Lymphangiioleiomyoma, urinoma
Cystic mass with pulmonary cysts	Lymphangiioleiomyoma
Cyst after trauma	
With high attenuation or intensity	Hematoma
With obstruction	Urinoma
Cyst with negative attenuation, history of radical lymphadenectomy	Lymphocele
Multilocular cystic mass, calcification, elongated shape, crossing retroperitoneal compartments	Lymphangioma
Cystic mass, calcification, no contrast enhancement, bone lesions, visceral involvement	Lymphangiomatosis
Cyst, history of pancreatitis, high amylase level	Pancreatic pseudocyst
Cyst in obese woman receiving hormonal therapy for menstrual irregularity	Müllerian cyst
Unilocular cyst in subdiaphragmatic space	Bronchogenic cyst
Multilocular cyst, thick septa, calcification, right lower quadrant	Pseudomyxoma retroperitonei
Presacral unilocular cyst	Epidermoid cyst
Presacral multilocular cyst	Tailgut cyst
Multilocular perianal cyst with history of anal fistula	Perianal mucinous carcinoma

The differential diagnosis of a predominantly cystic mass with areas of solid enhancement includes myxoid liposarcoma, schwannoma, and neurofibroma. A cystic mass with slow, progressive enhancement is typical of a lymphangioliomyoma (enhancement caused by slow lymphatic flow into the mass) or a urinoma (contrast-enhanced urine entering the urinoma). Lymphangioliomyoma is always associated with pulmonary cysts. A cyst that develops after trauma is likely to be hematoma or urinoma, with the former often having high-attenuation areas and the latter typically associated with urinary obstruction. A cyst with negative attenuation, particularly one occurring after lymphadenectomy or renal transplantation, is likely to be a lymphocele. A multilocular elongated cyst with faint calcification that crosses multiple retroperitoneal compartments is suggestive of a cystic lymphangioma, which when multiple and when associated with bone lesions and other visceral lesions is consistent with lymphangiomatosis. A cystic mass in a patient with a history of acute pancreatitis who has an elevated amylase level is indicative of a pancreatic pseudocyst. A cyst in an obese woman who is receiving hormonal therapy for irregular menstruation is likely to be a müllerian cyst. A cyst located in the subdiaphragmatic space is likely to be a bronchogenic cyst. A multilocular cyst with thick septa and calcifications that is located in the right lower quadrant is likely to be a pseudomyxoma retroperitonei, most likely caused by a ruptured mucocele of the appendix. A midline presacral cyst is likely to be an epidermoid cyst if it is unilocular or a tailgut cyst if it is multilocular. A multilocular perianal cyst in a patient with a history of an anal fistula is likely to be a perianal mucinous carcinoma.

Conclusions

Retroperitoneal masses can arise from various tissues and are a diverse group, including some rare neoplasms. CT and MR imaging are valuable in the evaluation of retroperitoneal masses, particularly in staging and the assessment of vascular invasion. Although a specific diagnosis

might be difficult to determine because of overlapping imaging appearances, the identification of certain characteristic imaging features, along with clinical and demographic information, may help in narrowing the differential diagnosis.

References

1. Neville A, Herts BR. CT characteristics of primary retroperitoneal neoplasms. *Crit Rev Comput Tomogr* 2004;45(4):247–270.
2. Koh DM, Moskovic E. Imaging tumours of the retroperitoneum. *Imaging* 2000;12(1):49–60.
3. Nishino M, Hayakawa K, Minami M, Yamamoto A, Ueda H, Takasu K. Primary retroperitoneal neoplasms: CT and MR imaging findings with anatomic and pathologic diagnostic clues. *RadioGraphics* 2003;23(1):45–57.
4. Nishimura H, Zhang Y, Ohkuma K, Uchida M, Hayabuchi N, Sun S. MR imaging of soft-tissue masses of the extraperitoneal spaces. *RadioGraphics* 2001;21(5):1141–1154.
5. Chesbrough RM, Burkhard TK, Martinez AJ, Burks DD. Gerota versus Zuckerkandl: the renal fascia revisited. *Radiology* 1989;173(3):845–846.
6. Korobkin M, Silverman PM, Quint LE, Francis IR. CT of the extraperitoneal space: normal anatomy and fluid collections. *AJR Am J Roentgenol* 1992;159(5):933–942.
7. Dodds WJ, Darweesh RM, Lawson TL, et al. The retroperitoneal spaces revisited. *AJR Am J Roentgenol* 1986;147(6):1155–1161.
8. Burkill GJ, Healy JC. Anatomy of the retroperitoneum. *Imaging* 2000;12(1):10–20.
9. Pereira JM, Sirlin CB, Pinto PS, Casola G. CT and MR imaging of extrahepatic fatty masses of the abdomen and pelvis: techniques, diagnosis, differential diagnosis, and pitfalls. *RadioGraphics* 2005;25(1):69–85.
10. Song T, Shen J, Liang BL, Mai WW, Li Y, Guo HC. Retroperitoneal liposarcoma: MR characteristics and pathological correlative analysis. *Abdom Imaging* 2007;32(5):668–674.
11. Ohguri T, Aoki T, Hisaoka M, et al. Differential diagnosis of benign peripheral lipoma from well-differentiated liposarcoma on MR imaging: is comparison of margins and internal characteristics useful? *AJR Am J Roentgenol* 2003;180(6):1689–1694.
12. Craig WD, Fanburg-Smith JC, Henry LR, Guerrero R, Barton JH. Fat-containing lesions of the retroperitoneum: radiologic-pathologic correlation. *RadioGraphics* 2009;29(1):261–290.
13. Hartman DS, Hayes WS, Choyke PL, Tibbetts GP. Leiomyosarcoma of the retroperitoneum and inferior vena cava: radiologic-pathologic correlation. *RadioGraphics* 1992;12(6):1203–1220.

14. Cuevas C, Raske M, Bush WH, et al. Imaging primary and secondary tumor thrombus of the inferior vena cava: multi-detector computed tomography and magnetic resonance imaging. *Curr Probl Diagn Radiol* 2006;35(3):90–101.
15. Kim EE, Valenzuela RF, Kumar AJ, Raney RB, Eftekari F. Imaging and clinical spectrum of rhabdomyosarcoma in children. *Clin Imaging* 2000;24(5):257–262.
16. Best AK, Dobson RL, Ahmad AR. Cardiac angiosarcoma. *RadioGraphics* 2003;23(Spec Issue):S141–S145.
17. Murphey MD, Walker EA, Wilson AJ, Kransdorf MJ, Temple HT, Gannon FH. Imaging of primary chondrosarcoma: radiologic-pathologic correlation. *RadioGraphics* 2003;23(5):1245–1278.
18. Taori K, Patil P, Attarde V, Chandanshive S, Rangankar V, Rewatkar N. Primary retroperitoneal extraskeletal mesenchymal chondrosarcoma: a computed tomography diagnosis. *Br J Radiol* 2007;80(959):e268–e270. <http://bjr.birjournals.org/cgi/content/full/80/959/e268>. Accessed June 5, 2010.
19. Ulasan S, Kizilkilic O, Yildirim T, Hurcan C, Bal N, Nursal TZ. Radiological findings of primary retroperitoneal synovial sarcoma. *Br J Radiol* 2005;78(926):166–169.
20. Song H, Koh BH, Cho OK, et al. Primary retroperitoneal synovial sarcoma: a case report. *J Korean Med Sci* 2002;17(3):419–422.
21. Prasad SR, Sahani DV, Mino-Kenudson M, et al. Neoplasms of the perivascular epithelioid cell involving the abdomen and the pelvis: cross-sectional imaging findings. *J Comput Assist Tomogr* 2007;31(5):688–696.
22. Kammen BF, Elder DE, Fraker DL, Siegelman ES. Extraadrenal myelolipoma: MR imaging findings. *AJR Am J Roentgenol* 1998;171(3):721–723.
23. Nguyen BD. Retroperitoneal extraadrenal myelolipoma: technetium-99m sulfur colloid scintigraphy and CT imaging. *Clin Nucl Med* 2007;32(2):135–138.
24. Casillas J, Sais GJ, Greve JL, Iparraguirre MC, Morillo G. Imaging of intra- and extraabdominal desmoid tumors. *RadioGraphics* 1991;11(6):959–968.
25. Castellazzi G, Vanel D, Le Cesne A, et al. Can the MRI signal of aggressive fibromatosis be used to predict its behavior? *Eur J Radiol* 2009;69(2):222–229.
26. Kreuzberg B, Koudelova J, Ferda J, Treska V, Spidlen V, Mukensnabl P. Diagnostic problems of abdominal desmoid tumors in various locations. *Eur J Radiol* 2007;62(2):180–185.
27. Dinauer PA, Brixey CJ, Moncur JT, Fanburg-Smith JC, Murphey MD. Pathologic and MR imaging features of benign fibrous soft-tissue tumors in adults. *RadioGraphics* 2007;27(1):173–187.
28. Rha SE, Byun JY, Jung SE, Chun HJ, Lee HG, Lee JM. Neurogenic tumors in the abdomen: tumor types and imaging characteristics. *RadioGraphics* 2003;23(1):29–43.
29. Hughes MJ, Thomas JM, Fisher C, Moskovic EC. Imaging features of retroperitoneal and pelvic schwannomas. *Clin Radiol* 2005;60(8):886–893.
30. Otal P, Mezghani S, Hassissene S, et al. Imaging of retroperitoneal ganglioneuroma. *Eur Radiol* 2001;11(6):940–945.
31. Singh KJ, Suri A, Vijjan V, Singh P, Srivastava A. Retroperitoneal ganglioneuroma presenting as right renal mass. *Urology* 2006;67(5):1085.e7–e8. [http://www.goldjournal.net/article/S0090-4295\(05\)01694-8/abstract](http://www.goldjournal.net/article/S0090-4295(05)01694-8/abstract). Accessed June 5, 2010.
32. Lonergan GJ, Schwab CM, Suarez ES, Carlson CL. Neuroblastoma, ganglioneuroblastoma, and ganglioneuroma: radiologic-pathologic correlation. *RadioGraphics* 2002;22(4):911–934.
33. Mukherjee JJ, Peppercorn PD, Reznick RH, et al. Pheochromocytoma: effect of nonionic contrast medium in CT on circulating catecholamine levels. *Radiology* 1997;202(1):227–231.
34. Bessell-Browne R, O'Malley ME. CT of pheochromocytoma and paraganglioma: risk of adverse events with i.v. administration of nonionic contrast material. *AJR Am J Roentgenol* 2007;188(4):970–974.
35. Varghese JC, Hahn PF, Papanicolaou N, Mayo-Smith WW, Gaa JA, Lee MJ. MR differentiation of pheochromocytoma from other adrenal lesions based on qualitative analysis of T2 relaxation times. *Clin Radiol* 1997;52(8):603–606.
36. Choyke PL, Hayes WS, Sesterhenn IA. Primary extragonadal germ cell tumors of the retroperitoneum: differentiation of primary and secondary tumors. *RadioGraphics* 1993;13(6):1365–1375.
37. Ueno T, Tanaka YO, Nagata M, et al. Spectrum of germ cell tumors: from head to toe. *RadioGraphics* 2004;24(2):387–404.
38. Gatcombe HG, Assikis V, Kooby D, Johnstone PA. Primary retroperitoneal teratomas: a review of the literature. *J Surg Oncol* 2004;86(2):107–113.
39. Keitoku M, Konishi I, Nanbu K, et al. Extraovarian sex cord-stromal tumor: case report and review of the literature. *Int J Gynecol Pathol* 1997;16(2):180–185.
40. Trabelsi A, Ben Abdelkarim S, Hadfi M, et al. Primary mesenteric Sertoli-Leydig cell tumor: a case report and review of the literature. *J Oncol* 2008;2008:619637. <http://www.ncbi.nlm.nih.gov/pmc/articles/PMC2648635/>. Published October 30, 2008. Accessed June 5, 2010.

41. Elsayes KM, Staveteig PT, Narra VR, Chen ZM, Moustafa YL, Brown J. Retroperitoneal masses: magnetic resonance imaging findings with pathologic correlation. *Curr Probl Diagn Radiol* 2007;36(3):97-106.
42. Dhillon MS, Rai JK, Gunson BK, Olliff S, Olliff J. Post-transplant lymphoproliferative disease in liver transplantation. *Br J Radiol* 2007;80(953):337-346.
43. Monill J, Pernas J, Montserrat E, et al. CT features of abdominal plasma cell neoplasms. *Eur Radiol* 2005;15(8):1705-1712.
44. Birjawi GA, Jalbout R, Musallam KM, Tawil AN, Taher AT, Khoury NJ. Abdominal manifestations of multiple myeloma: a retrospective radiologic overview. *Clin Lymphoma Myeloma* 2008;8(6):348-351.
45. Surabhi VR, Menias C, Prasad SR, Patel AH, Nagar A, Dalrymple NC. Neoplastic and nonneoplastic proliferative disorders of the perirenal space: cross-sectional imaging findings. *RadioGraphics* 2008;28(4):1005-1017.
46. Cronin CG, Lohan DG, Blake MA, Roche C, McCarthy P, Murphy JM. Retroperitoneal fibrosis: a review of clinical features and imaging findings. *AJR Am J Roentgenol* 2008;191(2):423-431.
47. Gottlieb R, Chen A. MR findings of Erdheim-Chester disease. *J Comput Assist Tomogr* 2002;26(2):257-261.
48. Veyssier-Belot C, Cacoub P, Caparros-Lefebvre D, et al. Erdheim-Chester disease: clinical and radiologic characteristics of 59 cases. *Medicine (Baltimore)* 1996;75(3):157-169.
49. Georgiades CS, Neyman EG, Francis IR, Sneider MB, Fishman EK. Typical and atypical presentations of extramedullary hemopoiesis. *AJR Am J Roentgenol* 2002;179(5):1239-1243.
50. Mesurole B, Sayag E, Meingan P, Lasser P, Duvillard P, Vanel D. Retroperitoneal extramedullary hemopoiesis: sonographic, CT, and MR imaging appearance. *AJR Am J Roentgenol* 1996;167(5):1139-1140.
51. Yang DM, Jung DH, Kim H, et al. Retroperitoneal cystic masses: CT, clinical, and pathologic findings and literature review. *RadioGraphics* 2004;24(5):1353-1365.
52. Wunderbaldinger P, Paya K, Partik B, et al. CT and MR imaging of generalized cystic lymphangiomatosis in pediatric patients. *AJR Am J Roentgenol* 2000;174(3):827-832.
53. Boyse TD, Jacobson JA. Case 45: cystic angiomatosis. *Radiology* 2002;223(1):164-167.
54. Levey DS, MacCormack LM, Sartoris DJ, Haghighi P, Resnick D, Thorne R. Cystic angiomatosis: case report and review of the literature. *Skeletal Radiol* 1996;25(3):287-293.
55. Marom EM, Moran CA, Munden RF. Generalized lymphangiomatosis. *AJR Am J Roentgenol* 2004;182(4):1068.
56. Yang DH, Goo HW. Generalized lymphangiomatosis: radiologic findings in three pediatric patients. *Korean J Radiol* 2006;7(4):287-291.
57. Abbott GF, Rosado-de-Christenson ML, Frazier AA, Franks TJ, Pugatch RD, Galvin JR. Lymphangiomyomatosis: radiologic-pathologic correlation. *RadioGraphics* 2005;25(3):803-828.
58. Maeda E, Akahane M, Inoue Y, et al. Delayed enhancement of pelvic lymphangiomyoma associated with lymphangiomyomatosis on MR imaging (2005: 9b). *Eur Radiol* 2005;15(12):2528-2531.
59. Pallisa E, Sanz P, Roman A, Majó J, Andreu J, Cáceres J. Lymphangiomyomatosis: pulmonary and abdominal findings with pathologic correlation. *RadioGraphics* 2002;22(Spec Issue):S185-S198.
60. Lee SA, Bae SH, Ryoo HM, Jung HY, Jang SB, Kum YS. Primary retroperitoneal mucinous cystadenocarcinoma: a case report and review of the literature. *Korean J Intern Med* 2007;22(4):287-291.
61. Kaku M, Ohara N, Seima Y, et al. A primary retroperitoneal serous cystadenocarcinoma with clinically aggressive behavior. *Arch Gynecol Obstet* 2004;270(4):302-306.

Imaging of Uncommon Retroperitoneal Masses

Prabhakar Rajiah, MBBS, MD, FRCR • Rakesh Sinha, MD, FRCR • Carlos Cuevas, MD • Theodore J. Dubinsky, MD • William H. Bush, Jr, MD Orpheus Kolokythas, MD

RadioGraphics 2011; 31:949–976 • Published online 10.1148/rg.314095132 • Content Codes: GI OI

Page 949

Of the primary retroperitoneal neoplasms, 70%–80% are malignant in nature, and these account for 0.1%–0.2% of all malignancies in the body (1,2).

Page 954

The presence of extensive necrosis in a retroperitoneal mass, with contiguous involvement of a vessel, is highly suggestive of leiomyosarcoma.

Page 958

Neurogenic tumors are seen commonly (*a*) along the sympathetic ganglia, which are located in the paraspinal region, and (*b*) in the adrenal medulla or the organs of Zuckerkandl (paraaortic bodies). Less commonly, neurogenic tumors occur in other sites, such as the urinary bladder, abdominal wall, bowel wall, or gallbladder (28).

Page 962

A fat-fluid (sebum) level and chemical shift between fat and fluid are pathognomonic.

Page 965

Retroperitoneal fibrosis is seen most commonly surrounding the infrarenal abdominal aorta and proximal common iliac arteries.